University of Zurich[UZH]

Department of Geography

Measuring plant traits — a comparison of imaging spectroscopy and a functional trait database

GEO 610 Master's Thesis

Remote Sensing Laboratories
Department of Geography
University of Zurich

Master Thesis December 31, 2016

Author: Basil Kraft
Matriculation-Nr: 09-932-013
E-Mail: basilkraft@gmail.com

Faculty Representative: Prof. Dr. Michael E. Schaepman
Supervisors: Prof. Dr. Michael E. Schaepman
PD Dr. Alexander Damm

Abstract

Plant functional traits are features of an individual impacting fitness indirectly via its impacts on growth, reproduction and survival. They became an important tool in modern ecology, offering the opportunity to quantitatively model terrestrial vegetation. Hence, the need for global, consistent plant trait data grows. In 2007, the TRY initiative has been launched with the aim to build a global *in situ* trait database (Kattge et al., 2011). But when it comes to large spatial scales, the *in situ* approach has its limitations though. Imaging spectroscopy and other remote sensing techniques have the potential to complement the field approach by contiguously mapping traits over large areas. Both approaches are successfully used to monitor plant traits, but up to date, no concept exist to merge them. The objective of this study is to compare the two approaches and discuss their limitations and convergence. Therefore, two traits, leaf chlorophyll (CHL) and leaf water content (LWC), are derived from imaging spectroscopy for a study area in Central Europe using vegetation indices (VIs). Via a species classification, a link between the traits and six predominant species is established. The same traits are extracted from the gap-filled TRY database for Europe. The trait distributions from the two sources were then contrasted. Intraspecific variations showed large differences, the imaging spectroscopy traits are much broader and vastly overlapping between species as opposed to the traits from the TRY dataset. It is concluded that the differences emerge from limited precision of imaging spectroscopy traits (especially associated to the VI approach) on the one hand, and biases in case of TRY on the other hand. The latter is supposedly mostly because of an artificial reduction of intraspecific variance due to sampling protocols and sparse sampling, limited to a number of distinct sites. To enable a better data-basis for future studies, imaging spectroscopy and airborne remote sensing in general can provide a link between *in situ* and satellite data or be integrated into gap-filling approaches.

Zusammenfassung

Plant functional traits beeinflussen die Fitness eines Individuums indirekt über deren Einfluss auf Wachstum, Reproduktion und Fortbestand. Sie sind mittlerweile eine wichtige Grundlage der modernen Ökologie, in der das quantitative Modellieren der terrestrischen Vegetation ein zentraler Bestandteil ist. Da eine solide Datengrundlage für globale Studien fehlte, wurde die TRY-Initiative 2007 gegründet, mit dem Ziel, diese Lücke zu schliessen. *In situ* Sampling stösst jedoch an seine Grenzen wenn es darum geht, eine globale Abdeckung zu erreichen. Bildgebende Spektoskopie (eng. Imaging Spectroscopy) und andere hochauflösende Fernerkundungsmethoden können verwendet werden, um Traits über grosse Flächen zu erfassen und haben damit das Potenzial, den *in situ* Ansatz zu ergänzen. Leider existieren bis heute keine konkreten Pläne, diese beiden Ansätze zusammenzuführen. Diese Studie soll die beiden Ansätze vergleichen und deren Grenzen sowie potenzielle Verbindungen diskutieren. Dazu werden zwei Traits, Blatt-Chlorpphylgehalt und Blattwassergehalt von Imaging Spectroscopy mittels Vegetationsindices für ein Studiengebiet in Zentraleuropa abgeleitet. Mittels Spezies-Klassifizierung kann dann eine Verbindung zu den sechs prädominanten Arten hergestellt werden. Die selben Traits werden von der TRY Datenbank abgeleitet, jedoch für ganz Euroa. Die Variabilität innerhalb und zwischen den Arten unterscheidet sich erheblich unter den Traits aus den beiden verschiedenen Quellen. Die Verteilungen der Imaging Spectroscopy Traits sind deutlich breiter und deren Überlagerung zwischen den Arten deutlich höher als diejenigen aus TRY. Dies ist einerseits auf die geringere Präzision bei der Messung von Traits via Imaging Spectroscopy (im Speziellen beim Verwenden von Vegetationsindices) zurückzuführen. Andererseits bestehen in TRY Lücken, die aus einem inkompletten Sampling von einer kleinen Anzahl von Orten sowie das verwenden von Sampling-Protokolle resultiert. Für eine bessere Datengrundlage für global orientierte Studien kann flugzeuggestützte Fernerkundung den Link zwischen *in situ* und satellitengestützter Fernerkundung herstellen oder verwendet werden, um gap-filling Ansätze zu unterstützen.

Table of Contents

List of Figures

List of Tables

List of Abbreviations

$ANCB_{650\text{-}720}$	area under continuum-removed curve normalized to the chlorophyll absorption band depth between 650 and 720 nm
aHPMF	advanced hierarchical probabilistic matrix factorization
APEX	airborne prism experiment
BHPMF	bayesian hierarchical probabilistic matrix factorization
CH	canopy height
CHL	leaf chlorophyll a&b content
CHM	canopy height model
DGVM	dynamic global vegetation model
DTM	digital terrain model
GIS	geographic information system
HWSD	harmonized world soil database
ITC	individual tree crown
LiDAR	light detection and ranging
LWC	leaf water content
NDWI	normalized difference water index
PCA	principal component analysis
PFT	plant functional type
RF	random forest
RMSE	root-mean-square error
RTM	radiative transfer model
SNR	signal-to-noise ratio
SVM	support vector machine
UAV	unmanned aerial vehicle
VI	vegetation index

1 | Introduction

The ongoing debate whether the variety of impacts of human activities on planet Earth legitimates the introduction of a new epoch, the Anthropocene (Waters et al., 2016; Lewis & Maslin, 2015; Steffen et al., 2007), illustrates the expansive implication of our actions on the environment. The consequences are far-reaching, from changes in climate (Meehl et al., 2007), loss of biodiversity (Sala et al., 2000) up to impacts on long-term geological processes (Crutzen, 2006), to name only a few. It is essential for us and future generations to monitor, understand and model the involved processes and impacts in order to make informed decisions in a fast changing world.

In the last decades, research has put more effort in studying the worlds vegetation, acknowledging its involvedness with the earth-system (Steffen et al., 2004), but also recognizing that humanity relays on ecosystem goods and services (Costanza et al., 1997). From rather simple models describing vegetation dynamics on a high level of abstraction and treating species or even communities as a discrete unit, more flexible and quantitative methods emerged (Díaz et al., 2016; van Bodegom et al., 2014). The trait-based approach, which bases upon measurement of features at individual level, allowing an individual to be "unique" rather than being categorized based on simplistic assumptions (Cadotte et al., 2011; Violle et al., 2007; McGill et al., 2006). This approach works on all levels of abstraction and from regional to global scale, but depends, however, ultimately on the availability of trait data. There exist two major methods to measure trait data, *in situ* sampling and remote sensing.

The *in situ* approach requires a direct access to the object of interest. This may include collecting leaves for later measurements or dimensioning an individual in the field. This method allows to take accurate measurements using standardized sampling protocols (Cornelissen et al., 2003). It may be feasible (yet laborious) to gather *in situ* data for regional studies, but rather unrealistic for global scales. Indeed, global studies need global data. In 2007, Kattge et al. (2011) started TRY, an initiative to compile regional *in situ* datasets into one single, global database. TRY has been used in a range of studies since then (a complete list is available online: `https://www.try-db.org/TryWeb/Publications.php`). The TRY database is extremely sparse, which can be partially overcome using gap-filling approach to fill the missing values statistically

(Schrodt et al., 2015). Nevertheless, TRY shows biases on different levels and a global coverage of plant traits using *in situ* techniques is unrealistic (Jetz et al., 2016).

Remote sensing is bases on measurement from distance. This incorporates a variety of platforms, ranging from small drones, helicopters and airplanes up to satellites orbiting the earth, carrying different sensors systems like spectroradiometers, laser- or radarbased systems. Therewith, data can be collected contiguously, covering regional scales with high resolution (meters) up to global scales, with a lower resolution of tens to hundreds of meters (Lillesand et al., 2008). Only a limited number of traits can be measured using remote sensing. Airborne LiDAR (light detection and ranging), for example, can be used to derive structural traits like plant height or crown dimension (van Leeuwen & Nieuwenhuis, 2010) but is rather insensitive to below-canopy traits like trunk volumes (Hilker et al., 2010). Imaging spectroscopy measures a range of wavelengths with a high spectral resolution on pixel basis and is capable of quantifying especially physiological and biochemical traits (e.g. leaf water, nitrogen or chlorophyll content) but is restricted to top-of-canopy (Homolova et al., 2013). The link to individuals can be done using species classification approaches (Martin et al., 1998). Satellites can cover global scales with high temporal resolution, however, they can measure only a limited number of traits due to the low *spectral* resolution and the link to species cannot be established because of the low *spatial* resolution (Homolova et al., 2013).

This thesis consists of a study (presented in Chapter 2) that will be submitted to *Remote Sensing of Environment*. The aims are to: i) derive high quality species specific vegetation index maps for a study site for the traits chlorophyll content (CHL) and leaf water content (LWC) using airborne imaging spectroscopy, ii) compare the traits to the respective traits from the gap-filled TRY database and iii) detect sources of possible mismatches of the traits and discuss convergence of the two approaches. In Chapter 3, the findings are briefly reflected.

2 | Measuring plant traits — a comparison of imaging spectroscopy and a functional trait database.

This chapter is based on:

Kraft, B., Damm, A. & Schaepman, M. E. (author list to be extended). Measuring plant traits — a comparison of imaging spectroscopy and a functional trait database.

To be submitted to:

Remote Sensing of Environment

Contribution:	
Design	60%
Materials & Methods	85%
Results & Conclusions	80%

Abstract

Plant functional traits are features of an individual impacting fitness indirectly via its impacts on growth, reproduction and survival. They became an important tool in modern ecology, offering the opportunity to quantitatively model terrestrial vegetation. Hence, the need for global, consistent plant trait data grows. In 2007, the TRY initiative has been launched with the aim to build a global *in situ* trait database (Kattge et al., 2011). But when it comes to large spatial scales, the *in situ* approach has its limitations though. Imaging spectroscopy and other remote sensing techniques have the potential to complement the field approach by contiguously mapping traits over large areas. Both approaches are successfully used to monitor plant traits, but up to date, no concept exist to merge them. The objective of this study is to compare the two approaches and discuss their limitations and convergence. Therefore, two traits, leaf chlorophyll (CHL) and leaf water content (LWC), are derived from imaging spectroscopy for a study area in Central Europe using vegetation indices (VIs). Via a species classification, a link between the traits and six predominant species is established. The same traits are extracted from the gap-filled TRY database for Europe. The trait distributions from the two sources were then contrasted. Intraspecific variations showed large differences, the imaging spectroscopy traits are much broader distributed and vastly overlapping between species as opposed to the traits from the TRY dataset. It is concluded that the differences emerge from limited precision of imaging spectroscopy traits (especially associated to the VI approach) on the one hand, and biases in case of TRY on the other hand. The latter is supposedly mostly because of an artificial reduction of intraspecific variance due to sampling protocols and sparse sampling, limited to a number of distinct sites. To enable a better data-basis for future studies, imaging spectroscopy and airborne remote sensing in general can provide a link between *in situ* and satellite data or be integrated into gap-filling approaches.

Keywords Functional traits, Imaging spectroscopy, Temperate forest, TRY

2.1 Introduction

The impact of global change on the biosphere involves a large array of consequences, one of it being loss of biodiversity (IPCC, 2014). Efforts to halt this irreversible trend were not successful up to date (Tittensor et al., 2014), even if the international community agrees on the importance of this task (Secretariat of the Convention on Biological Diversity, 2005). A decreasing diversity goes along with a loss of ecosystem functions, threatening the supply of essential goods and services (Cardinale et al., 2012). Numerous studies have shown that ecosystem functions can be linked directly to plant functional traits (de Bello et al., 2010; Díaz et al., 2007; Petchey & Gaston, 2006; Díaz & Cabido, 2001), which are the morphological, physiological or phenological features of an individual impacting fitness indirectly via its effects on growth, reproduction and survival (Violle et al., 2007). With the objective to understand and predict functional diversity in a changing environment, functional traits have been used in a large array of research fields. Hence, functional traits have become an important tool in a quantitative, more globally orientated ecology (Violle et al., 2014; Kattge et al., 2011; Lavorel et al., 2007; Cornelissen et al., 2003). Díaz et al. (2016), for example, used functional trait data to picture global functional diversity of vascular plants and link plant form and function to a limited set of trait combinations. Lavorel et al. (2007) see huge potential in functional traits to derive more representative plant functional types (PFTs), used to limit the complexity of global vegetation models. Others, like Scheiter et al. (2013) or van Bodegom et al. (2012) work towards fully trait-based and thus more flexible dynamic global vegetation models (DGVMs). More examples can be found in Cornelissen et al. (2003) and Kattge et al. (2011). However, these studies need a consistent, representative database, covering a wide range of traits from different species, regions and environmental conditions.

With the aim to establish such a global trait database, Kattge et al. (2011) launched the TRY initiative in 2007, a seminal project to merge existing plant trait databases into a global collection of field measurements and make them available for the scientific community. Up to date, TRY contains over 5 million records for 1100 traits and 100 000 plant species. However, TRY exhibits two major deficiencies. First, the dataset is extremely sparse, less than two percent

of the traits are measured per individual (Schrodt et al., 2015). Second, the individual plants are not selected randomly, which introduces a bias leading to a loss of representativity (Jetz et al., 2016).

The sparseness of TRY has been tackled using gap-filling approaches to predict missing entries (Swenson, 2014; Shan et al., 2012), culminating in a method called bayesian hierarchical probabilistic matrix factorization (BHPMF) proposed by Schrodt et al. (2015), that accounts for phylogeny and trait-trait correlations. With a mean performance of R^2=0.88 $\pm$ 0.085 for 13 selected traits, the method seems promising. Though, the sparseness of the selected traits (49.6-92.3) is not representative for the average sparsity of TRY, which is around 98%. And still, gap-filling methods can not correct for the bias present in the dataset, as they rely on the concept of the samples being a representative subset of the population, which may not be given. Jetz et al. (2016) visualised the "spatial and environmental data gap" for latitudinal regions and found that on average, only 2% of vascular plants have any trait measurements associated and that there is still a huge data gap in terms of taxonomical, geographical, environmental, temporal and functional representativity. This limits the range of questions that can be answered and could lead to wrong conclusions if biases are not being considered properly (Lindenmayer & Likens, 2013).

The existing gaps in TRY cannot be filled by solely putting more efforts in collecting field data. Field measurements are always limited through financial means and capacity limits and are prone to biases by nature (Schimel et al., 2015; Marvin et al., 2014). An approach with huge potential to complement the field-bases approach and reduce the mentioned deficiencies is remote sensing. Space-borne missions to monitor global vegetation exist, satellite products are used to monitor changes of vegetation type, cover (Turner et al., 2003; Friedl et al., 2002; Tucker & Townshend, 2000) and activity (de Jong et al., 2013) over time and are used as covariates in global biodiversity models (Pettorelli et al., 2016; Skidmore & Pettorelli, 2015; Jetz et al., 2012). However, they are not specialized on the task of mapping global plant trait variations (Jetz et al., 2016). On the other hand, airborne systems like imaging spectroscopy (Schaepman et al., 2009) and LiDAR (van Leeuwen & Nieuwenhuis, 2010) have reached a technological level that allows to measure traits with a high spatial resolution (Hilker et al., 2010; Kokaly et al., 2009; Ustin

et al., 2009) and link them to species via canopy classification approaches (Féret & Asner, 2013; Martin et al., 1998). Asner & Martin (2016) demonstrated this potential of imaging spectroscopy by linking canopy traits to species across numerous sites over the world.

However, imaging spectroscopy has limitations. The set of traits that can be derived is restricted to canopy- and leaf-level (which can, as has been demonstrated by Feilhauer et al. (2016), be partly overcome using trait-trait correlations), as light interacting with the upper canopy is measured (Homolova et al., 2013). Further, imaging spectroscopy measures are dependent on a variety of conditions like viewing angle that have to be controlled (Asner et al., 2015) and on factors disturbing the trait signal like canopy structure (Blackburn, 2007) and shadow effects (Damm et al., 2015) which introduce uncertainties. Imaging spectroscopy, as opposed to *in situ* sampling, measures traits at pixel basis. To establish a link between pixel and species, a resolution much smaller than the species dimension is needed. Even if large areas can be covered with this approach, the spatial extent and temporal resolution are limited (Homolova et al., 2013).

Both approaches, field measurements and remote sensing, have strengths and weaknesses. Still, no concrete plans exist to merge these approaches on a global scale even if the benefits are non-controversial. Local studies, comparing field measurements from the TRY database to remotely sensed traits are missing.

This study is an attempt to make a first step in this direction. We investigate in a regional study how imaging spectroscopy and *in situ* measurements, represented by the gap-filled TRY dataset, complement each other when coming from independent sources. Therefore, two physiological traits are derived for the site, being located in Central Europe: Leaf chlorophyll a&b content (CHL) and leaf water content (LWC), the ratio of leaf water to fresh mass, are estimated at maximum growing season via vegetation indices (VIs). Both VIs can be derived in high quality from multispectral imaging data (Homolova et al., 2013). Chlorophyll a&b allows to draw conclusions about plant-environment interactions (Blackburn, 2007) and are key elements in the photosynthesis (Grimm, 2001), which is an important driver of ecosystem services like climate regulation or carbon sink (Garbulsky et al., 2013). As a measure of canopy water condition, LWC is a useful indicator of carbon uptake and plant transpiration (Stimson et al., 2005). Also,

light detection and ranging (LiDAR)-based canopy height (CH) is used to assess the heterogeneity of plants in the datasets, as the TRY database has been restricted to full-grown plants. This traits are combined with a species classification of the study site, which provides a link between pixel-based trait measurements and species. The VI maps are then rescaled to fit the trait values present in the TRY database, in which all three traits are present or can be derived from. We then investigate the traits from the different sources, their distributions and co-variation, which allows to draw conclusions about the two approaches and their convergence.

2.2 Materials

2.2.1 Study area

The Lägern (47.48N, 8.40E, 866 m a.s.l.) is an eastern foothill of the Jura mountain range located in Switzerland, northwest of Zurich (see Fig. 9 in in Apendix A). The hill ridge of about 10 km length is almost entirely covered with managed temperate forest. The site shows a high diversity in terms of species, age and diameter distribution. In the western part, the forest is dominated by Ash (*Fraxinus excelsior*), Sycamore (*Acer pseudoplatanus*) and European beech (*Fagus sylvatica*). In the east, European beech, Norway spruce (*Picea abies*) and, to a lesser extent, Silver fir (*Abies alba*), are predominant. Other, less common species to be found at the site are Linden (*Tilia cordata*), Oak (*Quercus robur*) and Elm (*Ulmus glabra*). At the south-facing slope, a 300 x 300 m plot is located (further referred to as P1, see Fig. 1), consisting of mature, full grown trees. For this area, reference tree species data is available in the form of polygons delineating individual tree crowns (ITCs). A further subplot (P2) of 800 x 800 m, located in the east, shows high species diversity and is used to visualize results in more details. For a more extensive description of the study site, we refer to Eugster et al. (2007).

2.2.2 The TRY database

The TRY initiative (Kattge et al., 2011) has been launched in 2007 with the objective to make global trait data available for the research community in a consistent way. A variety of databases have been compiled, and TRY is still growing. Up to date, the database contains over 5 million

records for 1 100 traits and 100 000 plant species. Nearly half of the records are geo-referenced (`http://www.try-db.org`, December 30, 2016).

The TRY data (version June 2015) used in this study has been received pre-filtered and gap-filled. The pre-filtering was done as described in Kattge et al. (2011): The trait-space was limited to non-juvenile plants and plants grown under natural environmental conditions. Illogical values have been removed. Then, a robust outlier detection has been applied. The data has been gap-filled using BHPMF (Schrodt et al., 2015). BHPMF is briefly summarized in Appendix D. The gap-filling was done for the global dataset, based on 86 652 entries for leaf dry mass, 31 898 for leaf fresh mass and 19 222 for leaf chlorophyll content per leaf area.

2.2.3 Individual tree crown data

An ITC map (shown in Appendix 12) representing single tree crowns for plot P1 was used to train and do a species classification of the Lägern site. The tree species map was derived from UAV data, which was collected on 21 October, 2013 at a flight height of 270 m above ground. The UAV data, consisting of 174 rectified images, was co-registered to a canopy height model derived from airborne laser scanning data, resulting in a merged dataset with a spatial resolution of 8 x 8 cm. Crown shapes have been derived using an ITC detection approach. Mixed crowns and polygons containing more than two tree crowns were removed manually. The ITCs were associated with tree species in a field campaign.

2.2.4 LiDAR data

A canopy height model (CHM), derived from LiDAR data (further referred to as CHM_{LiDAR}), has been provided by Schneider et al. (2014). Full-waveform LiDAR data (1550 nm wavelength) was gathered under leaf-on (August 1st 2010) and leaf-off (April 10th) conditions, using RIEGL LMS-Q680i sensor in the first and RIEGL LMS-Q560 sensor in the second mission. The sensors were mounted on a helicopter. The data, having a footprint of 0.25 m and a point density of 20 points per m^2 in leaf-off and 40 points per m^2 under leaf-on conditions, was used to generate the CHM_{LiDAR}. First, a digital terrain model (DTM) was derived by selecting and interpolating ground return echoes. The CHM_{LiDAR} was then calculated by subtracting the DTM from the first

echoes (representing top of canopy) in the leaf-on dataset. The resulting map was registered to the Swiss national grid CH1903+ and resampled to a spatial resolution of 2 x 2 m. The reported uncertainty in height is up to $\pm$4 m. For more details regarding flight mission, dataset and product generation, we refer to Schneider et al. (2014).

2.2.5 Imaging spectroscopy data

The spectral data was acquired using APEX (airborne prism experiment), an airborne dispersive pushbroom imaging spectrometer (Schaepman et al., 2015). Three scenes were captured under clear sky conditions on April 24, June 21 and August 24 2015. Each scene consist of 284 spectral bands covering the wavelength-range from 399 to 2432 nm with a spectral sampling interval of 2.5-14.1 nm and a full width at half maximum ranging from 3.3 to 14.2 nm. The flight height of 4.5 km above sea level resulted in a ground pixel size of around 2 x 2 m for all three missions. Postprocessing of the APEX data was done by performing spectral, geometric and radiometric calibration (Hueni et al., 2013) as well as geo-rectification and atmospheric correction (Richter & Schläpfer, 2002; Schläpfer & Richter, 2002). The three APEX scenes were image-to-image co-registrated to the LiDAR datasets using ENVI v5.3 (Exelis Visual Information Solutions, 2015).

2.3 Methods

2.3.1 Preparation of TRY dataset

The gap-filled TRY dataset as provided was filtered in terms of species and geographic extent. Species not occurring on the Lägern site (see Eugster et al. (2007) for complete list) were dropped. Also, species being underrepresented in the tree species map covering subplot P1 (introduced in subsection 2.2.3), were excluded from the dataset. Further, the geographic region was limited from -8 to 25° in longitude and 40 to 55° in latitude, centering the dataset around the study area. In this step, non-georeferenced records were dropped. The area has been chosen rather large, ensuring that enough samples from different sites remain in the dataset. To verify the comparability of the Lägern site to a much larger area, covering several climatic regions, the

trait-ranges have been compared between different climatic zones (see Appendix 13 for more details). The selected species and the distributions of the observations are showed in Fig. 3.

Leaf chlorophyll content per leaf area [g m^{-2}] (CHL_{TRY}) and canopy height [m] (CH_{TRY}, also called plant height) are present in the gap-filled TRY dataset, while leaf water content [%] (CHL_{TRY}), the relative weight of water inside a leaf compared to the total weight, was derived from leaf fresh mass [g] and leaf dry mass [mg] as:

$$LWC_{TRY} = 1 - \frac{Leaf_{drymass}}{1000 * Leaf_{freshmass}} \tag{1}$$

2.3.2 Tree species classification of Lägern

A tree species classification for the Lägern site is performed to establish the link between VIs and species. The ITC map is used as ground truth and the three APEX scenes as explanatory data. Classification of forest canopy using imaging spectroscopy bases on the principle that different species have a characteristic spectral fingerprint that is expressed in the measured spectrum (Martin et al., 1998). The classification is performed using support vector machines (SVMs). SVMs are well suited for high dimensional, collinear settings with a low number of training samples and have been found to yield good results in species classification tasks using high resolution imaging spectroscopy data (Melgani & Bruzzone, 2004; Mountrakis et al., 2011). Inspired by Demir & Ertrk (2009), a spatial hierarchical approach has been chosen for classification, increasing the likelihood of neighboring pixels to belong to the same species as its surrounding pixels and thus, reducing the heterogeneity of the resulting species map. Pixels classified with low reliability were rejected. This conservative approach has been chosen due to validation data not being available outside subplot P1.

The ITCs were rasterized to exactly match the imaging spectroscopy data. Pixels covered to less than 95% by a single species were dropped in order to retain pure pixels to avoid a mixture of different species or of vegetation and background in a pixel (Fig. 12 in Appendix C). The SVM model is tuned on the original resolution of 2 x 2 m using 10-fold cross-validation. This has been done with the R package e1071 (Meyer et al., 2015), which allows for probability predictions

(based on LIBSVM, Chang & Lin (2011)). A radial kernel has been chosen because we want data points lying outside the data clusters in the feature-space to have a low classification certainty (see Appendix 11). The trained model is then applied on the original data-cube with 2 x 2 meter resolution (level 1) and a version down-sampled by factor 2 (level 2) using average function. Each pixel of level 1 is restricted to belong to one of the species occurring at the corresponding pixel of level 2 or its 8-neighbors. If none of the classes has a probability larger than a probability threshold p, the pixel is excluded as supposed to be a mixed pixel, a species not being part of the training dataset, or an atypical individual (e.g. young or unhealthy). Finally, the candidate class with the highest probability is assigned.

The probability threshold p is chosen based on the following criteria: (i) The accuracy (rate of correct classification) and Cohen's Kappa (Cohen, 1960) must be as large as possible ensuring the most robust prediction possible. (ii) A significant amount of pixels must remain in the final classification, containing pixels of all species of interest. (iii) The remaining pixels should be distributed over the whole site to represent the variability across the Lägern.

2.3.3 Deriving vegetation index maps of Lägern

Mapping of plant traits using imaging spectroscopy can be done using either physical or empirical models. Physical models, not considered in this study, base upon radiative transfer models (RTMs), which have the capability to simulate light absorption and scattering inside canopies as well as biophysical and -chemical properties of the leaves. Empirical models link the measured spectral signal to traits, most often by using VIs that have been defined empirically. Without a link to field measurements, VIs are relative quantities (Homolova et al., 2013). The reliability of VIs depends on using high quality sensors providing high signal-to-noise ratio measurements, focusing on dense vegetation (Asner et al., 2015) and controlling of influencing factors like viewing geometry and conditions (Richter & Schläpfer, 2002) and irradiance and shadow effects (Damm et al., 2015). Other factors like leaf structure and orientation, surface characteristics, moisture content and woody elements have an influence on the measurement as well and potentially impact the accuracy of VIs (Blackburn, 2007).

Relative trait maps for CHL_{APEX}, LWC_{APEX} and LAI_{APEX} are derived from the APEX June scene.

The LAI is used for postprocessing, which is subject to the next section. CHL_{APEX} is calculated using area under continuum-removed curve normalized to the chlorophyll absorption band depth between 650 and 720 nm ($ANCB_{650\text{-}720}$), as found in Malenovský et al. (2013), LWC_{APEX} via normalized difference water index (NDWI), described by Gao (1996). The LAI_{APEX} is calculated using an empirical function following Heiskanen (2006).

$$ANCB_{650-720} = \frac{\frac{1}{2}\sum_{j=1}^{n-1}(\lambda_{j+1}-\lambda_j)(1-\rho_{j+1}+1-\rho_j)}{1-\frac{R_b}{R_c}} \quad (2)$$

$$NDWI = \frac{R_{860}-R_{1240}}{R_{860}+R_{1240}} \quad (3)$$

$$LAI = 2.41 * 10^{-4} e^{10.83*(R_{860}-R_{670})/(R_{860}+R_{670})} \quad (4)$$

In formulas 2-4, R is the reflectance at a given wavelength, denoted as subscript. Rb is the reflectance at the wavelength of maximum absorption, R_c, the reflectance of continuum line at wavelength of maximum absorption. λ_j is the wavelength of band j, ρ_j continuum removed reflectance at band j, n is the number of spectral bands.

2.3.4 Postprocessing of the vegetation index maps

The VI maps were postprocessed to increase reliability and make the data consistent with the gap-filled TRY dataset. Applied steps include a) correcting the indices for shadowing-effects and b) dropping pixels of non-dense vegetation and removing pixels representing juvenile plants. Step a) increases the quality of the VI maps while step b) was performed for to remove ground, understory and mixed pixels as well as reducing the dataset to pixels representing grown trees. This step was necessary to be consistent with the TRY database, where juvenile plants have been removed before gap-filling.

Shadow-effect correction is a crucial step to improve VIs quality (Damm et al., 2015). Pixels being directly illuminated by the sun have a high signal-to-noise ratio (SNR), resulting in a high VI quality. Shaded pixels are an artifact of the atmospheric correction and receive high amounts of diffuse irradiance, which lowers the SNR and thus, the quality of the VI. For the correction of

shadow-effects, an illumination map for the APEX June scene was created. The training data was prepared by selecting 300 pixels from the scene randomly (restricted to forest). For each of these pixels (P), a nearby pixel (if possible from the same tree crown) that is in cast shadow (P_{sh}) and one being fully illuminated (P_{sun}) is selected and the spectrum is extracted from the APEX scene. The spectra (S) of each of these three pixels is averaged individually using arithmetic mean. The illumination intensity (I_p) was calculated as:

$$I_P = \frac{mean(S_P) - mean(S_{P_{sh}})}{mean(S_{P_{sun}}) - mean(S_{P_{sh}})} \tag{5}$$

The illumination map was then derived using linear SVM regression with the training data as ground truth, and the spectral data as explanatory variables. The resulting map, shown in Figure 1, is histogram stretched and scaled to values from 0 to 1. As a compromise between a pure signal and a sufficient amount of pixels, representing the variability of the traits at the study site, pixels with a lower illumination intensity than 0.5 were removed. This threshold is chosen by inspecting the LOESS smoothed relationship between shadow and VI, shown for CHL_{APEX} in Figure 2. It exhibits a nearly linear relationship and a constant variance above the illumination intensity of 0.5. The VI not shown in the figure (LWC_{APEX} & LAI_{APEX}) show a very similar behavior. The pixels not being rejected are corrected for the shadow effect; The LOESS fit was subtracted from the VI values and the mean of the smoothed line from illumination 0.5-1 is added again (Figure 2, bottom).

As a next step, pixels not covering full-grown trees were filtered out using the CHM_{LiDAR}. All pixels with $CHM_{LiDAR}<5$ m were removed. As the LiDAR data was acquired in 2010 and the analysis is based on 2015 data, we expect some changes in the canopy height. The height changes for the Lägern site from 2010 to 2014 have been quantified by Schneider et al. (2015): The mean height change was reported to be 0.3 m $\pm$ 0.2, caused by tree cutting and growth. Discarding regions where young trees grew up to a height above 5 m means rejecting some useful pixels. Contrariwise, accepting pixels where trees have been cut after 2010 possibly introduces some additional variation coming from juvenile trees. Finally, pixels showing an $LAI_{APEX}<2$ were discarded. The index maps are intersected with the tree species classification derived in section 2.3.2. This step further improves quality and pureness of the remaining pixels as the classification

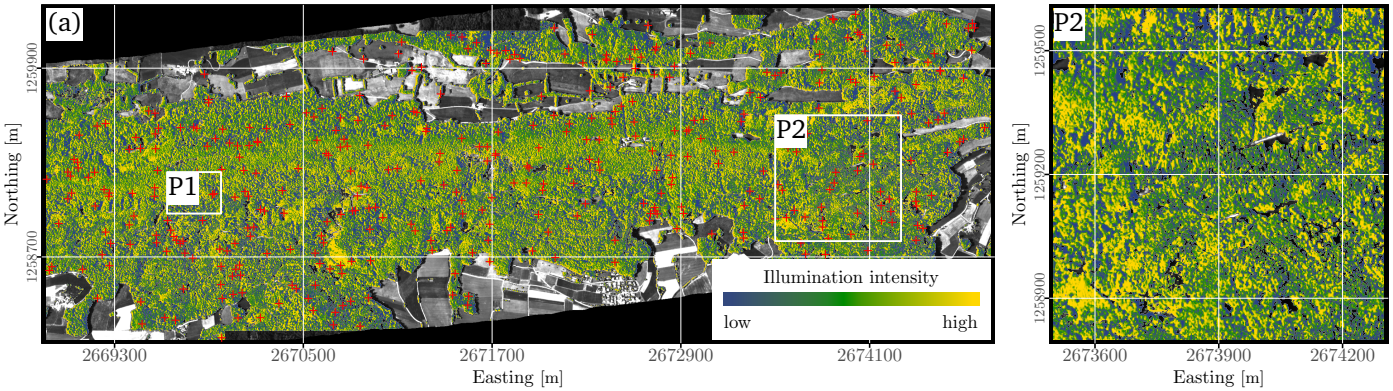

Figure 1: Map of Lägern showing illumination intensities (I_p), derived from APEX June scene. The training data is created by randomly select 300 pixels (+) and choosing a pixel in full shadow and full sun from the same tree crown. The illumination intensity was then calculated as a function of the selected pixels spectra. The training data is used to train a linear SVM on the spectral data and deriving an illumination map for the Lägern site.

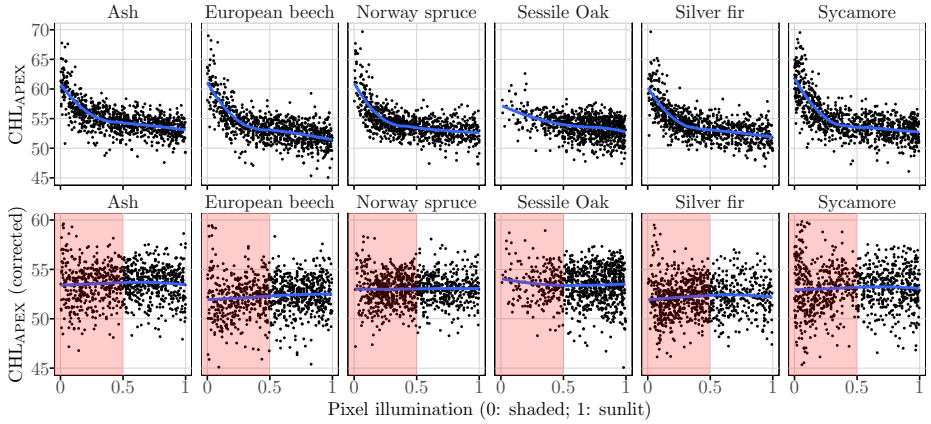

Figure 2: The top Figure shows the relationship between CHL_{APEX} and illumination intensity, which takes values from 0 (shaded) to 1 (sunlit). The blue line is the LOESS smoothed curve. The bottom Figure shows the CHL_{APEX} after correction for illumination effects. The red boxes show the part being removed from the dataset. The cut-off at illumination lower than 0.5 is a compromise between omitting shaded pixels, where the accuracy of the index is lower, and keeping enough pixels per species in the dataset to cover as much of the variability as possible. After correction, the shadow effect can be neglected.

implicitly filters for the same criteria: A high classification certainty is likely to be assigned to pure pixels (not being a mixture of multiple species or vegetation and soil) and moreover, pixels similar to the training pixels, which did not include juvenile plants.

Finally, CHM_{LiDAR}, was filtered using a 3 x 3 moving window with maximum function to set pixels to the nearby local maximum. This has been done to be consistent with the TRY database,

where the plant height at highest point is given. The resulting map was masked with the VI maps.

2.3.5 Rescaling vegetation indicess

The traits CHL_{APEX} and LWC_{APEX}, as derived from VIs, are relative quantities, while the TRY database contains measurements in absolute physical units. To be able to compare these measures in terms of species-wise co-variation and intraspecific differences, the VIs were rescaled. As no calibration data was used, a method mapping the minimum (f_{min}) and maximum (f_{max}) summary statistics from the VI to the absolute traits from TRY was applied. This was achieved by performing linear scaling of the values as:

$$VI_{scaled} = a * VI + b \tag{6}$$

with

$$a = \frac{f_{max}(T) - f_{min}(T)}{f_{max}(VI) - f_{min}(VI)} \tag{7}$$

$$b = f_{min}(VI) * \frac{f_{max}(T) - f_{min}(T)}{f_{max}(VI) - f_{min}(VI)} + f_{min}(VI) \tag{8}$$

The appropriate summary statistics is selected following theoretical consideration, supported by analyzing the stability of the summary statistic across different climatic zones (Fig. 13).

2.4 Results

2.4.1 TRY dataset

A set of species has been selected from the gap-filled TRY dataset. For each species, the number of samples and the number of distinct sites is reported in Table 1. The spatial distribution of the species, shown in Figure 3, reveals large spatial gaps in the TRY dataset at hand. Some species like Ash, Silver fir and Sycamore are underrepresented, while others, like Sessile oak and European beech are present in higher numbers. The most species investigated are sampled from a relatively small number of distinct sites.

Table 1: The table shows the tree species that have been selected for this study. The number of samples per species and distinct sites per species are displayed. A site is considered as distinct if the observation locations do not fall inside a grid of 1 x 1°.

Species name	Species type	Number of observations	Number of distinct sites
Ash	deciduous	128	15
European beech	deciduous	621	54
Norway spruce	conifer	517	39
Sessile oak	deciduous	820	21
Silver fir	conifer	113	14
Sycamore	deciduous	84	8

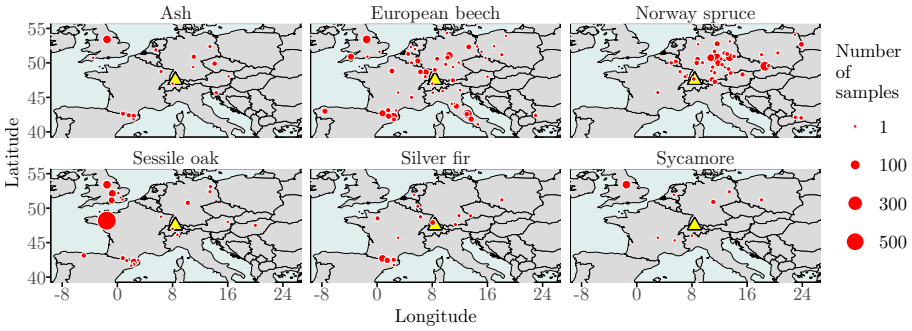

Figure 3: Geographical distribution of gap-filled TRY records per species. The observations have been aggregated and counted on a 1 x 1° grid. The Lägern study site is marked in yellow. Only a few samples are within the immediate vicinity of the study site.

2.4.2 Tree species classification

Figure 4 shows the criteria i & ii, introduced in section 2.3.2, in relation to threshold p. These criteria can only be validated inside subplot P1, as ground truth data is missing outside. This is a reason why p has been chosen very conservatively with $p = 0.875$, resulting in an accuracy of 0.93 ± 0.02, Cohen's Kappa of 0.83 ± 0.03 and 36% coverage, meaning that 64% of the pixels were removed. The spatio-hierarchical approach poses an improvement of about 3% in terms of Accuracy and Cohen's Kappa, compared to a more simplistic method which does not include the neighborhood restriction. In fact, this restriction does discard some additional pixels rather than changing the classification. Criterium iii, the spatial distribution of the remaining

pixels, is evaluated visually based on the final classification to the Lägern and a selected close-up area (P2), shown in Figure 5. The patterns appear to be homogeneously distributed and clumped, corresponding to individual or groups of tree crowns. Compared to Eugster et al. (2007), Sycamore is largely underrepresented in the west, while Silver fir is overrepresented in the East. The dominance of European beech seems legitimate.

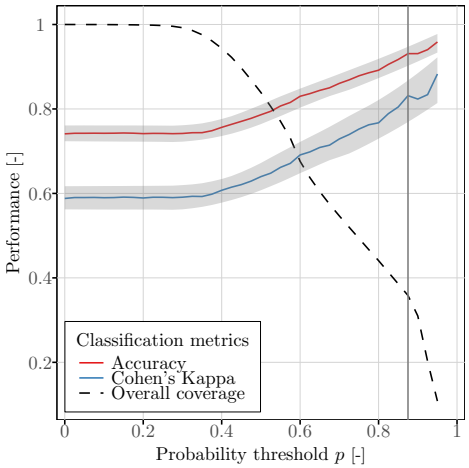

Figure 4: Species classification metrics in relationship to the probability threshold p. Pixels with a lower classification certainty than p are discarded. The classification metrics, accuracy and Cohen's Kappa and their standard deviation are derived using 10-fold cross-validation. The overall percentage of pixels remaining in the Lägern site when applying the threshold decreases continuously.

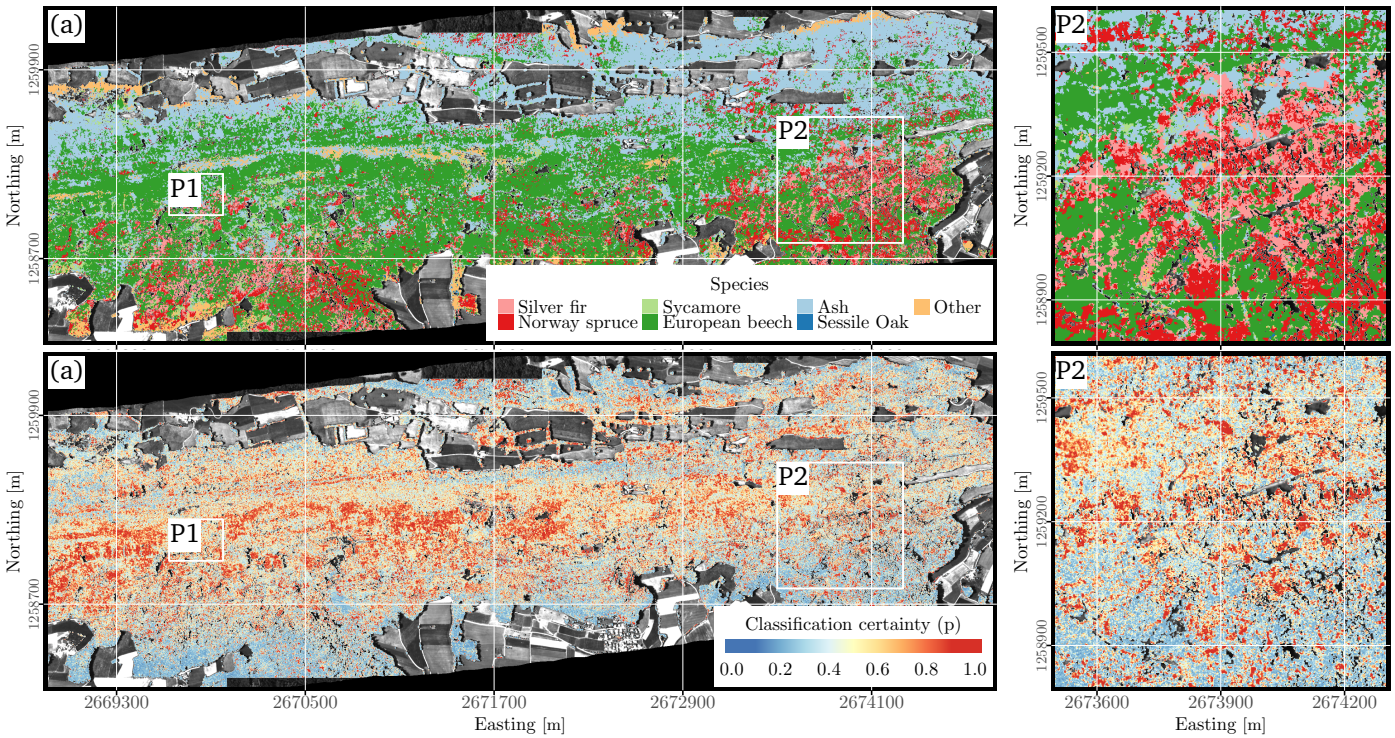

Figure 5: Species classification map of Lägern. Figure (a) shows the species classification of the Lägern site. The classification is based on training data available for plot P1. Linear SVM was trained and applied using all three APEX scenes. Figure (b) represents the classification certainty p. Subplot P2 shows a high species diversity, containing both, coniferous and deciduous trees. For further analysis, all pixels with p<0.875 are discarded.

2.4.3 Vegetation index maps of Lägern

CHL_{APEX} and LWC_{APEX} for the Lägern site were derived from the APEX June scene using common VIs. Postprocessing, which included correcting for shadow effects, excluding non-dense vegetation and juvenile plants below a height threshold, yielded high-quality VI maps. The shadow-corrected CHL_{APEX} and LWC_{APEX} as well as CHM_{LiDAR} are shown in Figure 6.

CHL_{APEX} shows no relationship to the insolation, coming from West, after shadow correction. Variations occur in small-scale patches, but also in larger dimensions. The northern region of the scene, being dominated by Ash, shows higher values of leaf chlorophyl content. The LWC_{APEX} values are distributed more homogeneously over the scene. The insolation seems to have an influence on the leaf water content, even after shadow-correction. This might be related to bad performance of the VI or with the irradiance drying out the leaves at top of canopy, which motivated the removal of pixels with illumination intensities below 0.5. LAI_{APEX}, used for post-processing, is shown in the Appendix 15. After removing pixels with an illumination intensity lower that 0.5 shadow effects were no longer visible.

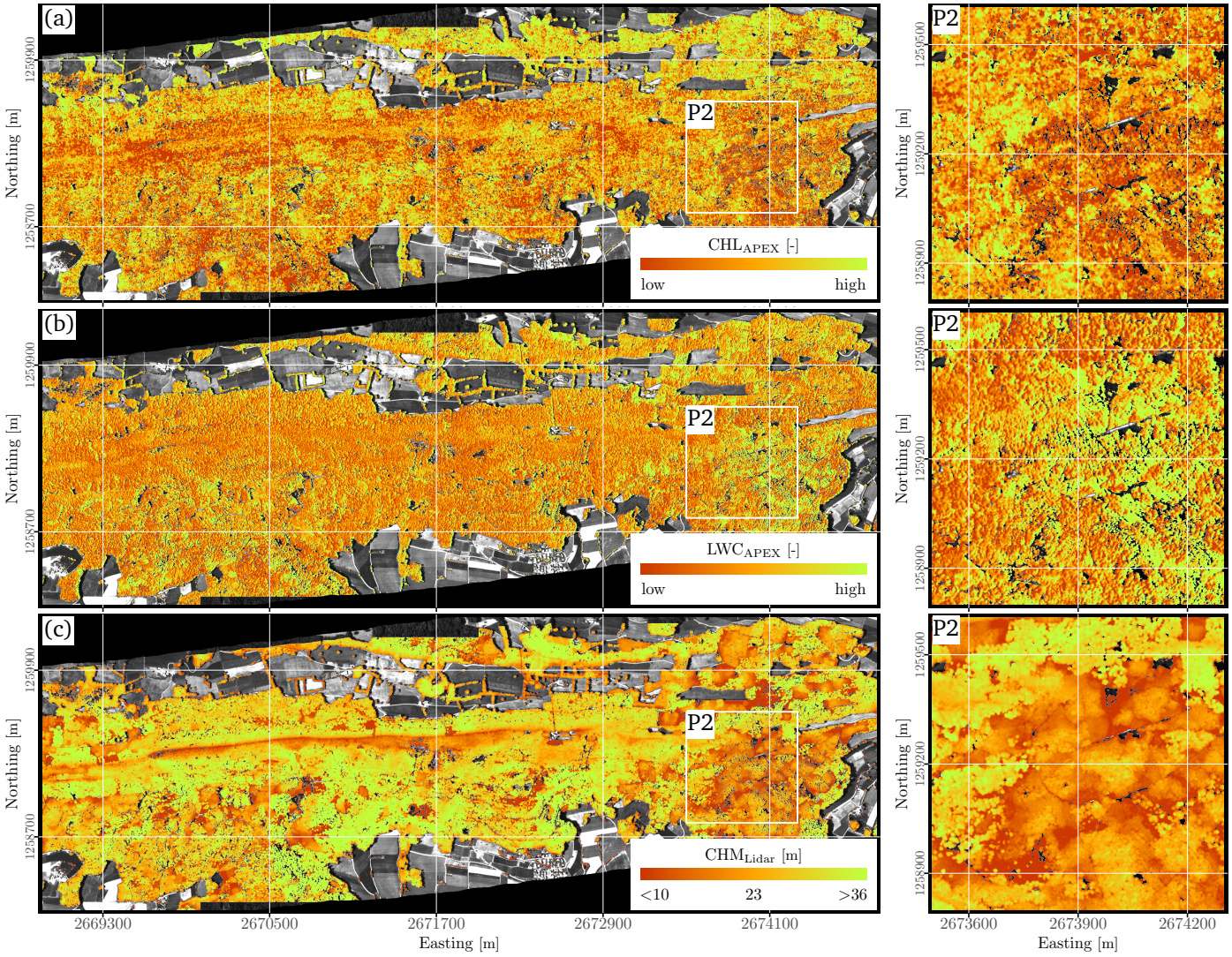

Figure 6: Trait maps of Lägern, showing (a) relative CHL$_{APEX}$, (b) relative LWC$_{APEX}$ and (c) CHM$_{LiDAR}$. The maps a and b, derived from APEX data, were corrected for shadowing effects. CHM$_{LiDAR}$ is derived from LiDAR. The plots on the righthand side show the close-up view of subplot P2.

2.4.4 Comparing remotely sensed traits to field observations

To compare VIs to the field measurement, an appropriate summary statistic had to be selected to input into formula (6) introduced in Section 2.3. We decided to use per-species summary statistics, because they represent the interspecific rather than overall variations, as we suppose the VIs to be not highly precise, but in principle accurate measurements of the traits. The mode was selected due to this measure being the most stable across different climatic regions (See Appendix 13). This suggests that the true range of per-species modes at the Lägern corresponds to those across Europe.

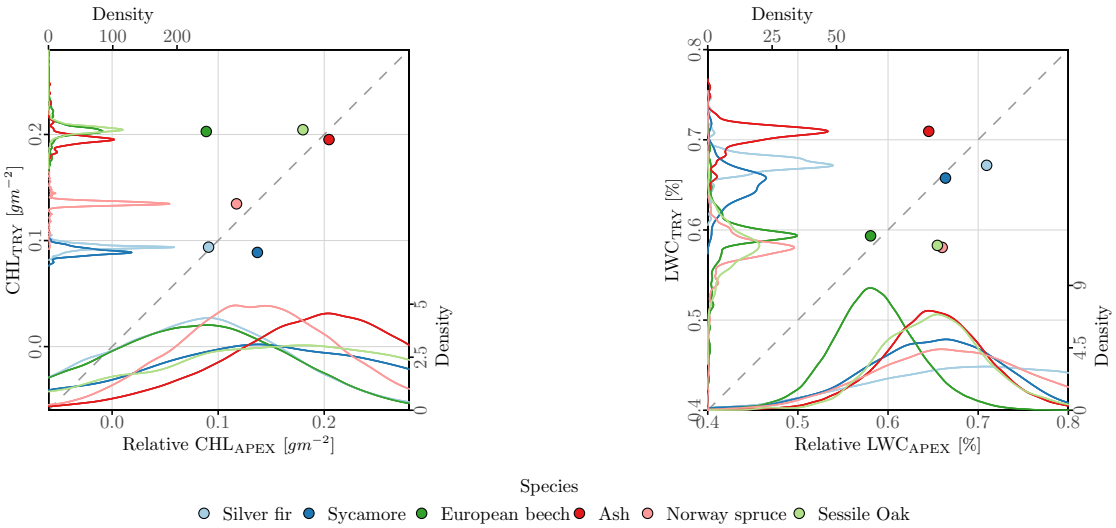

Figure 7: Cross comparison of TRY traits (Europe) versus VIs (Lägern) for CHL and LWC. The VIs have been scaled by mapping the minimum and maximum mode across all species to the respective values of the TRY traits. The points correspond to the mode of the distributions. The densities of the TRY traits are depicted along the y-axis, the relative traits from imaging spectroscopy along the x-axis.

Per-species distributions and co-variations of the APEX indices and the TRY traits are shown in Figure 7. The distributions of the traits from both sources are unimodal and unskewed. The most striking difference, present in the two plots, are the peaked distributions in TRY, opposed to the strongly overlapping and flat distributions of the VIs. The variation explained by the species (which is the intraspecific variance divided by the total variance) is 94% for CHL_{TRY}, but only 26% in case of CHL_{APEX}. The modes of CHL_{TRY} and CHL_{APEX} are co-varying except

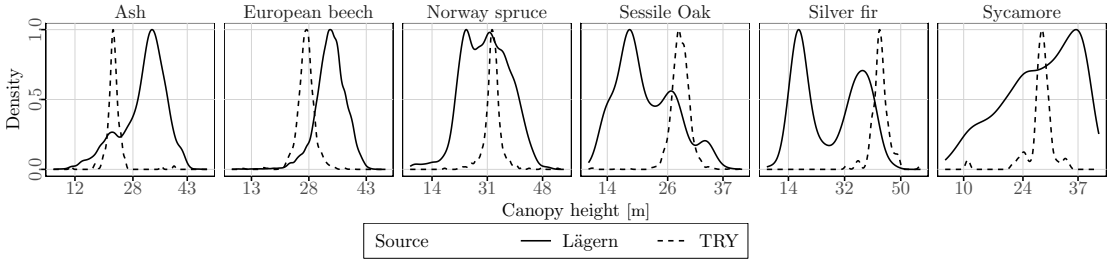

Figure 8: The Figure shows the canopy height derived plant height of Lägern vs plant height in TRY for selected species. The estimation of canopy height *in situ* is done via direct measurement or via allometric rules, deriving the height from other metrics (Cornelissen et al., 2003). The height of the Lägern trees is derived from a CHM_{LiDAR} by applying a focal maximum filter to go from canopy to plant height. This is a simple approach. However, it gives a valid (yet rough) representation of the plant heights at the site. The species in TRY have been selected following sampling protocols and have been further limited preliminary to applying gap-filling, which explains the unnatural hight distributions. It is unclear to what extent the reduction of trait space impacts the variability of other trait distributions. The plant heights at the Lägern site are limited to trees above 5 m, which is an attempt to be consistent with the TRY database, where juvenile plants have been removed. The distribution represent the afforestation at the site, some species like Silver fir show two highly distinct peaks of high-grown individuals of around 40 m and a second one at ca. 20 m, representing young stands and being the result of afforestation. Contrariwise, the European beech shows a more natural distribution.

for European beech, which takes high values in TRY, but low values in APEX. The variation in LWC_{TRY} is explained by 58%, those of LWC_{APEX} to 30% by the species. The modes of LWC are slightly co-varying.

The variabilities of the TRY traits are not significantly related to the number of samples present in the dataset. Norway spruce and European beech, for example, do not show substantially larger variation than species having less samples, like Sycamore. The relation has been tested using simple linear regression of standard deviation versus number of samples and resulted in $p=0.176$ in case of CHL and $p=0.1266$ for LWC.

To give an intuition for the limited diversity in the gap-filled TRY dataset, CHM_{TRY} and CHM_{LiDAR} are compared in Fig. 8.

2.5 Discussion

2.5.1 Representativity of this study

The TRY database represents the largest source of plant traits currently available. The gap-filling approach used to fill the missing values is state-of-the-art and has been proved to yield good results (Schrodt et al., 2015). Europe has the highest sampling density in the dataset (Kattge et al., 2011) and thus, our study might not be representative for other areas, where substantially less samples are available.

The imaging spectroscopy data covers a relatively small, but highly diverse area. Even if other study sites might show different trait variabilities, the findings can be extended to other areas in Europe, as the basic principles (e.g. remote sensing versus *in situ*) and mechanisms (e.g. disturbing factors, sampling gaps) are inherent to this methods.

This study focuses on six species, which were selected to correspond to the predominant species at the Lägern site. Species underrepresented in one of the datasets were dropped. However, the findings might be valid for other tree species, as further discussion is not limited to these species in particular. This also applies to other traits than the two selected in this study, as long as they can be derived from imaging spectroscopy.

2.5.2 Imaging spectroscopy vs in situ observations

The imaging spectroscopy based data covers a small subset of the TRY data used in this study. Thus, the intraspecific variability of the traits is expected to be much smaller in reality. However, the comparison of the imaging spectroscopy and *in site* traits draws a different picture, which is, as we argue here, a result of the different measurement and sampling methods. The distributions are assessed taking first a remote sensing, and then the TRY perspective.

From the perspective of remotely sensed traits, the CHL_{TRY} distributions do underestimate the variation for all species and the overlapping among them. The main cause for intraspecific variation are the genetic variation and phenotypic plasticity (Pigliucci, 2001). The genetic variation determines the phenological plasticity, how an individual can react on environmental conditions. Thus, the existing variability of a trait is a function of the genotype and the en-

vironmental conditions, including climate and influences from other plants, animals or human activity. The per-species distributions of CHL_{TRY} suggest a very low plasticity and genetic variability over different environmental conditions, which is also visible in the comparison across climatic regions (Fig. 13). LWC_{TRY} exhibits larger intraspecific variance and larger overlapping of the distributions.

The probable underestimation of the intraspecific variations can have different reasons: An incomplete sampling, for example, caused by the use of standardized protocols. This can lead to a low overlapping of traits among species (Violle et al., 2012). As an example, we refer to Cornelissen et al. (2003), who established a sampling protocol for plant traits used to tackle large-scale questions. They propose to sample from robust, well grown plants located in well illuminated environments. For selection of leaves for later weighting of dry and fresh mass, which we use to derive LWC_{TRY}, it is suggested to select young leaves exposed to full sunlight, some hours after sunrise and before sunset. For sampling of the photosynthetic pathway, selection of fully expanded leaves from adult plants exposed to full sunlight is recommended. This sampling strategy extremely limits the intraspecific variation, as a tree crown consists of a highly diverse set of leaves regarding age, health status and exposure to sunlight. However, we don not know which sampling approaches have been used in the numerous smaller sampling cmapaigns, providing the data for the TRY database. A further reason is an incomplete sampling possibly leading to a bias (Jetz et al., 2016). Our study showed that the species samples originate from a limited number of distinct sites, which might reduce the intraspecific variability. Further, the selection of individuals at these sites may not be randomized, as this could demand a considerable extra effort (e.g. hard to reach areas) or not be in the interest of the local study. Finally, in the pre-filtering step, juvenile plants were removed, which can further reduce the variability.

Viewed from the TRY perspective, the VIs show very large variations and strongly overlap between species. The distribution of some species is even nearly congruent (e.g. CHL_{APEX} of European beech and Silver fir). This would imply a strong phenotypic plasticity of the species' genotypes (expecting the genetic variability to be limited at the study site). We suppose the large intraspecific variances of the VIs (compared to the *in situ* measurements) to have two major reasons.

First, imaging spectroscopy does not measure the traits of interest directly but rather the light that has interacted with the canopy (Kokaly et al., 2009; Ustin et al., 2009). The reflectance of the vegetation is not only influenced by the leaf properties, but also by scattering mechanisms inside the canopy, background and non-leaf material. Malenovský et al. (2013) showed that CHL_{APEX} dependent little on LAI and performs on deciduous and conifer trees. Contrariwise, LWC_{APEX} depends strongly on LAI, dry matter content and leaf structure (Ustin et al., 2004). The indices were corrected for shadow effects and restricted to dense vegetation only to reduce those and other disturbing factors. However, the handling of these factors is limited when using VIs (Homolova et al., 2013). Thus, VIs are considered to be a valid, but not very precise measurement.

Second, the link to species or leaf is not given when using imaging spectroscopy. However, the link from pixel to species can be established using species classification. In this study, training data is based on a small patch (P1), being populated by old, full-grown trees. The Lägern study site, however, is much more diverse in terms of species and age. As the quality of the species classification is hard to assess outside subplot P1, only pixels with high classification certainty made it into the final dataset, which is expected to increase the classification reliability substantially. A link between the VIs and single leaves cannot be made. A signal in a single pixel is an integral over leaves of different age, health status, orientation and exposure to sunlight, which is a substantial difference to field measurements.

The co-variation of the species-wise modes of the two sources is little conclusive. A minimal connection between the values may exist, but the strong overlapping (and for some species nearly congruent) distributions of the VIs suggest a high randomness of the results: Considering the number of possible uncertainties related to imaging spectroscopy and the VI approach in particular, small biases (e.g. species-specific measurement dependency, species classification) would have a high impact on the co-variation. Nevertheless, other studies have shown that deriving plant traits by using imaging spectroscopy is possible (Asner et al., 2015; Homolova et al., 2013).

The large differences in intraspecific variance are a product of the measurement methods, the sampling strategies and true differences in trait variations. While *in situ* measurements are highly

precise and accurate, imaging spectroscopy is prone to different factors reducing the precision, of which some can be controlled and others not. To express this in numbers, we refer to Asner et al. (2015), who performed a large-scale study in South America to assess the capability of imaging spectroscopy to measure canopy traits. Using more advanced techniques than the VI approach, the reported R^2 between the *in situ* and imaging spectroscopy observations of CHL and LWC were 0.7 and 0.49, respectively. This gives an impression of what is to expect from state-of-the-art imaging spectroscopy approaches.

The fundamental differences in sampling methods between *in situ* and imaging spectroscopy highly accounts for the differences in intraspecific variance. Imaging spectroscopy is not designed to gather selective trait information. It can map — and this is one of ist strengths — large areas (although limited to the canopy) and cover local trait variability including plants and leaves of different state (e.g. young and old, stressed, healthy). Contrariwise, field campaigns are in general not designed to cover traits from a broad variety of local conditions but rather sampling from specified leaves (e.g. young, exposed to full sunlight) and plants (full-grown, healthy) which allows to compare like with like around the globe. This leads to an underestimation of the local trait variability.

2.5.3 Bridging the gap

Imaging spectroscopy and airborne remote sensing in general is an approach that can map functional traits over large areas at species level. It is, however, not yet fully operational and standardized. The number of traits that can be gathered is limited and the expected accuracy is — depending on the application — adequate or not. Thus, imaging spectroscopy is not the one and only solution to the present lack of representative global plant trait data, but can be a part of it.

Asner et al. (2015) use imaging spectroscopy together with airborne LiDAR to map large, hard-to-reach areas, mainly focusing on tropical forests, where *in situ* samples are sparse. The approach, however, is stand-alone and does not include links to external datasets like TRY. A more integrative approach is envisioned by Díaz et al. (2016), who outlined a global biodiversity observatory linking *in situ* observations to satellite data and argued that remote sensing in

general can bridge some of the existing gaps in TRY. According to the authors, this allows to bring biodiversity observations to global coverage with temporal repeated measurements. In the proposed system, imaging spectroscopy, combined with LiDAR, could provide a link between the *in situ* and satellite data. However, a satellite mission matching the observatory requirements does not exist yet.

A feasible integration of *in situ* and airborne remote sensing could base upon the gap-filling technique. BHPMF relies on the principle that the taxonomic hierarchy is connected to trait similarity and that trait-trait co-variations are transmittable to regions where only less samples (or none) are present. This relationships could be investigated using airborne remote sensing. Further, biases present in TRY can be detected, as for example in this study, whereof a possible under-estimation of intraspecific variance emerges. As neither taxonomical similarities nor trait-trait co-variations are modeled explicitly and possible biases are not considered in BHPMF, the model would have to be extended.

Schrodt et al. (2015) tested the extension of BHPMF to out-of-sample predictions using environmental variables (climate and soil data) to model the intraspecific variance, calling it advanced hierarchical probabilistic matrix factorization (aHPMF). However, aHPMF did perform similar to BHPMF (tests of intraspecific trait modeling using environmental variables has been briefly tested in Appendix H). Imaging spectroscopy can reveal relationships between traits and environment variables and test their generalizability for under-sampled regions.

This, however, are only a few applications of (airborne) remote sensing for functional biodiversity assessment. For an extensive discussion of other approaches, including functional, taxonomical and structural biodiversity, we refer to Lausch et al. (2016).

2.6 Conclusion and outlook

Our study took a first look at the convergence of traits from imaging spectroscopy and *in situ* observations from independent sources. It has been shown that the species-wise trait distributions are vastly different, which is a demonstration for the potential of a fusion of the approaches. The co-variation of the traits is viewed critically; a correlation has been detected, which has, however, to be investigated further using more advanced methods to derive trait data

from imaging spectroscopy. We reason that this mismatch is introduced by i) the limited precision and accuracy of the vegetation indices, ii) sampling biases present in the *in situ* data and iii) an artificial reduction of the variance due to the use of sampling protocols.

Imaging spectroscopy can be used to detect and fill this and other gaps, as stand-alone approach mapping plant traits in hard-to-reach regions, as link between *in situ* and satellite data or integrated into gap-filling approaches, for example.

As a first evidence of a possible bias in the TRY database towards an underestimation of intraspecific trait variability is given, we suggest the use of RTMs for the derivation of canopy traits from imaging spectroscopy in order to increase the precision of the trait values. Also, this would allow to differentiate between inter- and interspecific variability (which has been done in this study based on a simplistic assumption), as derivation of absolute trait values is possible. The set of traits could be extended, also to LiDAR-based traits. Finally, a more sophisticated species classification method incorporating LiDAR data can increase the reliability of further studies.

3 | Synthesis

Plant trait data is the fundament to understand global vegetation dynamics. We have discussed two different approaches to acquire plant trait data, *in situ* sampling and imaging spectroscopy. The approaches are based on different principles and have their strengths and weaknesses. *In situ* observations are prone to biases and will never reach a spatial and temporal coverage that would be needed to map existing biodiversity and monitor the ongoing changes. Sampling protocols often reduce the trait variability artificially. Still, it is the most reliable source for functional trait measurements directly associated to individuals. Imaging spectroscopy and other remote sensing techniques can be used to overcome this issues, as stand-alone approach mapping plant traits in hard-to-reach regions, as link between *in situ* and satellite data or integrated into gap-filling approaches, for example.

The TRY database is a big step in the right direction. With it, consistent *in situ* data is made publicly available for the scientific community. With time, the database will grow and thus become more representative. On the other hand, more and more satellite data is made publicly available. This intensifies collaboration of remote sensing and biodiversity community (Turner et al., 2015). Unfortunately, this is not the case for imaging spectroscopy and LiDAR data. Usually, the data is used in local studies for basic research and access is restricted to a limited number of people. Making the data available for everyone is not enough: The community has to agree on consistent methods leading to comparable datasets.

To enforce a global biodiversity observatory, as envisioned by Jetz et al. (2016), the technical basis should be outlined and implemented, such that contributors can start to supply their data. Other than the current state of TRY, we would encourage a more spatially orientated approach — a geographic information system (GIS) —, linking trait data of all different sources and dimensions. This would facilitate the handling of spatial data in different formats (raster, vector, point) and allow to extract specific datasets (extent, temporal range, species etc.) for further analysis. A further concern regarding TRY in the current state is the missing date and time associated to each observation. This would allow to monitor changes over time and would be important for the integration with remote sensing data.

A | Study area

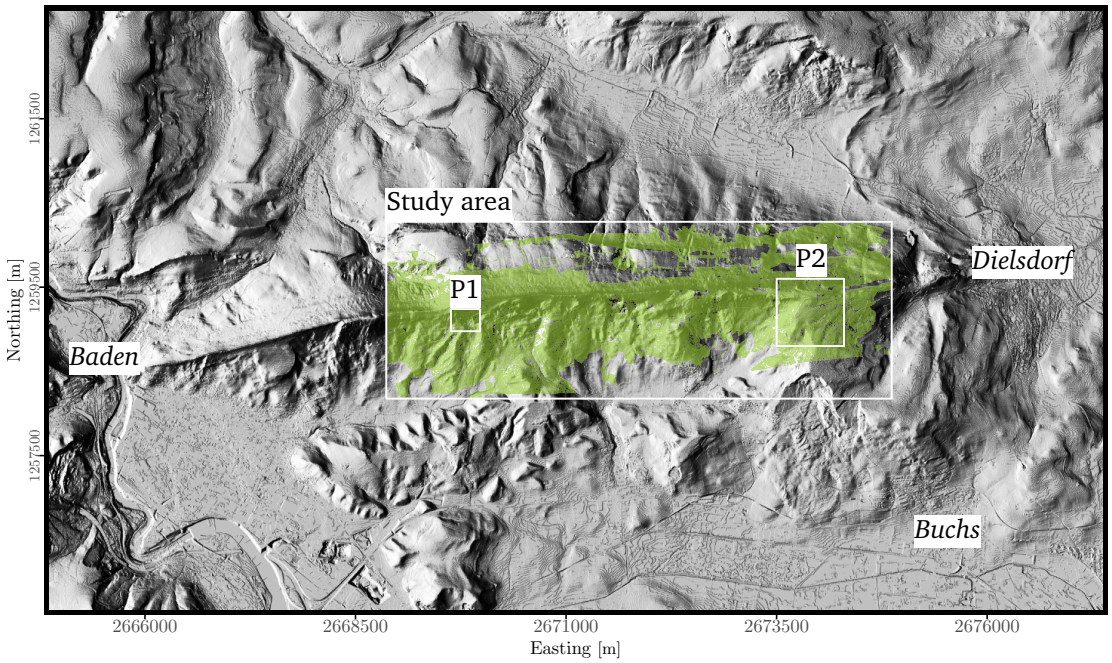

Figure 9: The Lägern is located northwest of Zurich. The ridge spans 10 km from Baden in the West to Dielsdorf in the East of the map. The study site is highly divers in terms of topography, containing flat to very steep areas. The analysis on the site is restricted to the forest at the study area (marked in green). Species data for subplot P1 has been used to do the species classification of the site. Subplot P2 has been chosen to validate classification and VIs at a higher zoom level. The hillshade based on a digital terrain model in the background of the map has been derived from swissALTI^{3D} of the Swiss Federal Office of Topography (Swisstopo, Switzerland).

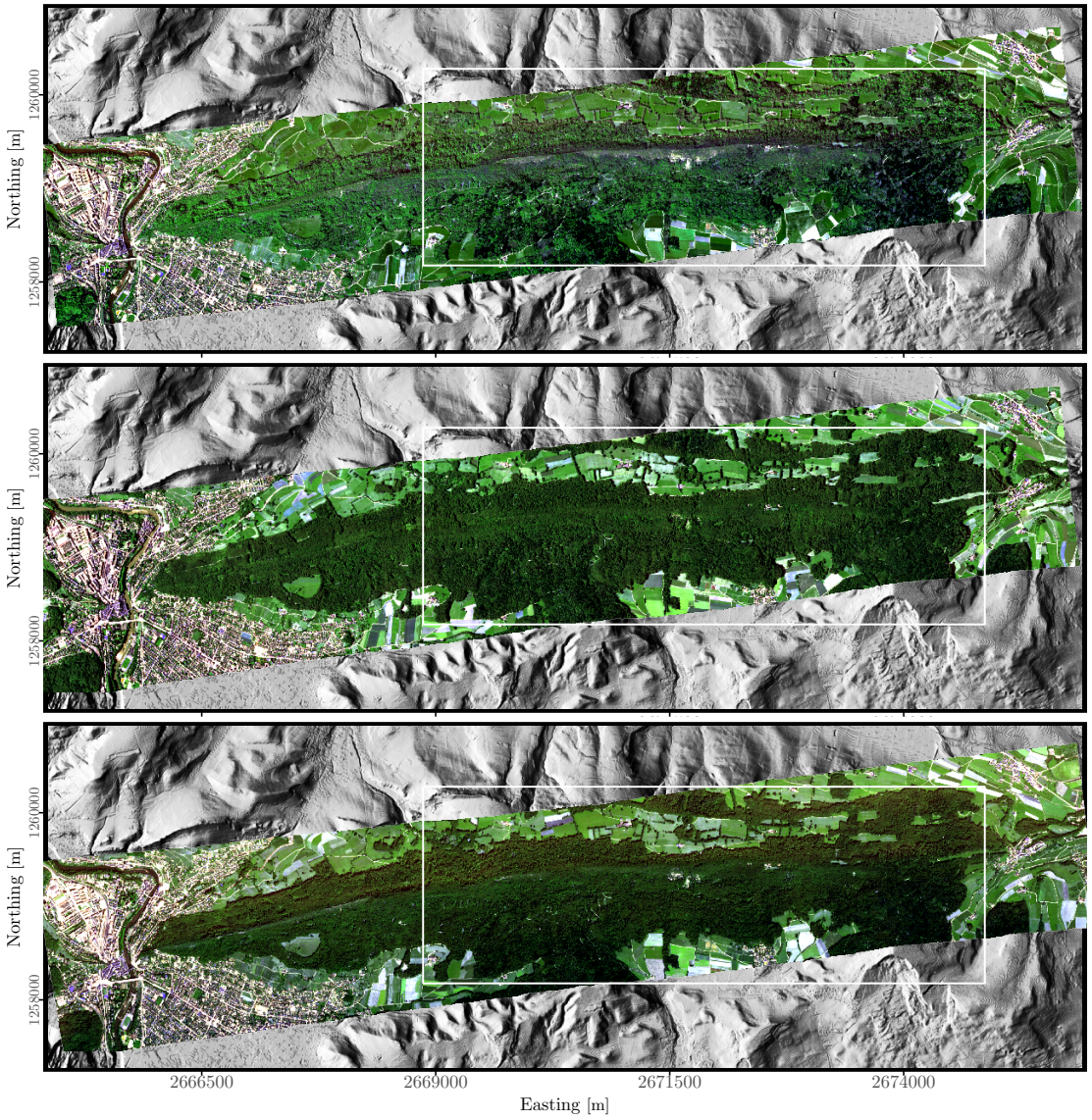

Figure 10: True-color representation of the APEX scenes showing the Lägern site. The top scene was captured on April 21, the middle scene on June 24 and the bottom scene on August 21, 2015. The white box shows the study area for which traits have been derived from the June scene. The hillshade based on a digital terrain model in background of the map has been derived from swissALTI^{3D} of the Swiss Federal Office of Topography (Swisstopo, Switzerland).

B | SVM kernel selection

Even if linear SVM is much faster and performed similar to a SVM with radial kernel, the radial method has been chosen. The training dataset is available for an area that is probably not entirely representative for the Lägern. When choosing linear SVM, shifts in the spectrum over different viewing or insolation angles and other factors would be likely to result in high classification certainties for pixels lying not inside the point cloud of the training set in the feature-space. Also, species not being part of the training set or living under different conditions can be assigned to training species with high certainty. A radial kernel can solve this problem, as Figure 11 illustrates.

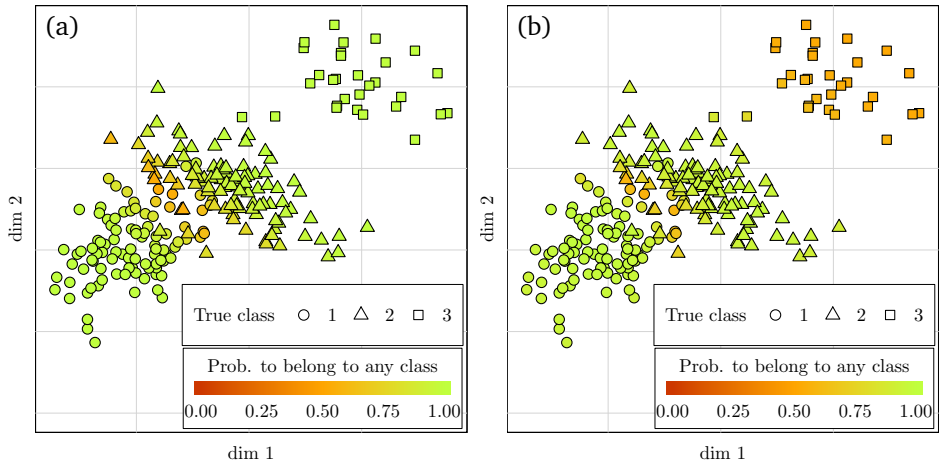

Figure 11: The figure illustrates the choice of a radial kernel for species classification. In the example, two classes, 1 & 2, are used to train the SVM model. In the case of a linear SVM (a), class 3 gets assigned to class 2 with a probability of nearly 1. The models is very confident about this, as there is no ”competing” class nearby. Figure (b) shows that, thanks to the radial kernel, class 3 has a low probability to belong to any of the training classes.

C | Tree crown data

Figure 12 shows the ITC polygons and the rasterized version. Species with a low number of pixels associated have been dropped. The map is used as training data for species classification of the Lägern site. The polygons cannot represent overlay of crowns of different species, thus, mixed crowns result in mixed pixels, which adds a small uncertainty to the data. However, the reliability of the dataset is considered to be high, as the classification assignment of the species is none in the field where such problems can be considered.

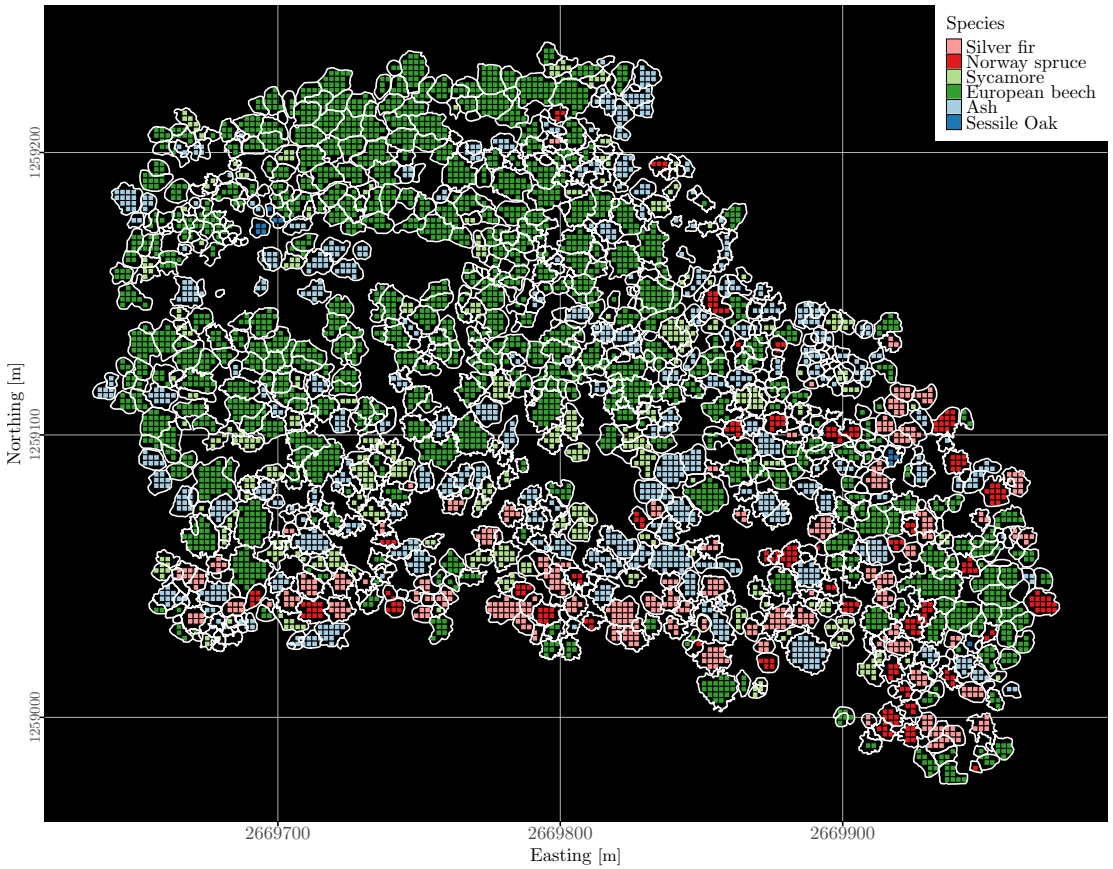

Figure 12: The original ITC data is shown as white polygons. In the raster representation, pixels that not covered by 95% or more by the same species are dropped in order to obtain pure pixels. The rasterized data is used for species classification of the Lägern site.

D | Bayesian hierarchical probabilistic matrix factorization

In this appendix, the concept of bayesian hierarchical probabilistic matrix factorization (BHPMF) is briefly summarized following Schrodt et al. (2015). BHPMF is a tool to fill sparse matrices using the hierarchical structure inherent in the data that allows to quantify uncertainty of the predicted values. The hierarchical structure is given by the taxonomy (individual, species, genus, family, phylogenetic group). BHPMF sequentially works on the different hierarchical levels, being represented by the single trait measurements in case of individual level, and by the mean values per group (e.g. per species, at species level) at the other hierarchical levels. A matrix at one of these levels is then expressed using the inner product of two latent matrices, consisting of orthogonal vectors that minimize the deviance from the data, which is, as Schrodt et al. (2015) point out, similar to principal component analysis (PCA). The latent matrices are used as prior for the next neighboring level to find the optimal solution iteratively. The parameters are found using Gibbs sampler.

E | TRY across climatic regions

Figure 13 shows the differences of CHL_{TRY} and LWC_{TRY} across different climatic regions. Two findings relevant to this study emerge from this plot: The geographic subset of the TRY database is chosen large, ensuring that enough samples per species are retained. The trait ranges are very stable over the different climatic regimes. A large range of values, with a lot of outliers (e.g. for European beech in Cfb climate) are related to large sample sizes. The Lägern study site, located on in Cfb, bordering Dfb, should be represented by the selected geographic subset. This means, in theory, we can expect the traits in the Lägern site to be covered by the distributions of the traits of the larger region and not lying outside. The second conclusion is that the scaling of the Lägern VIs should be done using the mode of the distributions. Other scaling methods, like mapping quantiles of the VIs to those of the TRY database are critical, as this procedure implicitly assumes that the variance in the Lägern site is the same as over the large Europe area. The mode was preferred over mean and median, as the mode is more stable across different climatic conditions. The assumption is that the mode values in TRY and the VIs covering the Lägern represent the true range of modes and is best suited to do the scaling of the VIs.

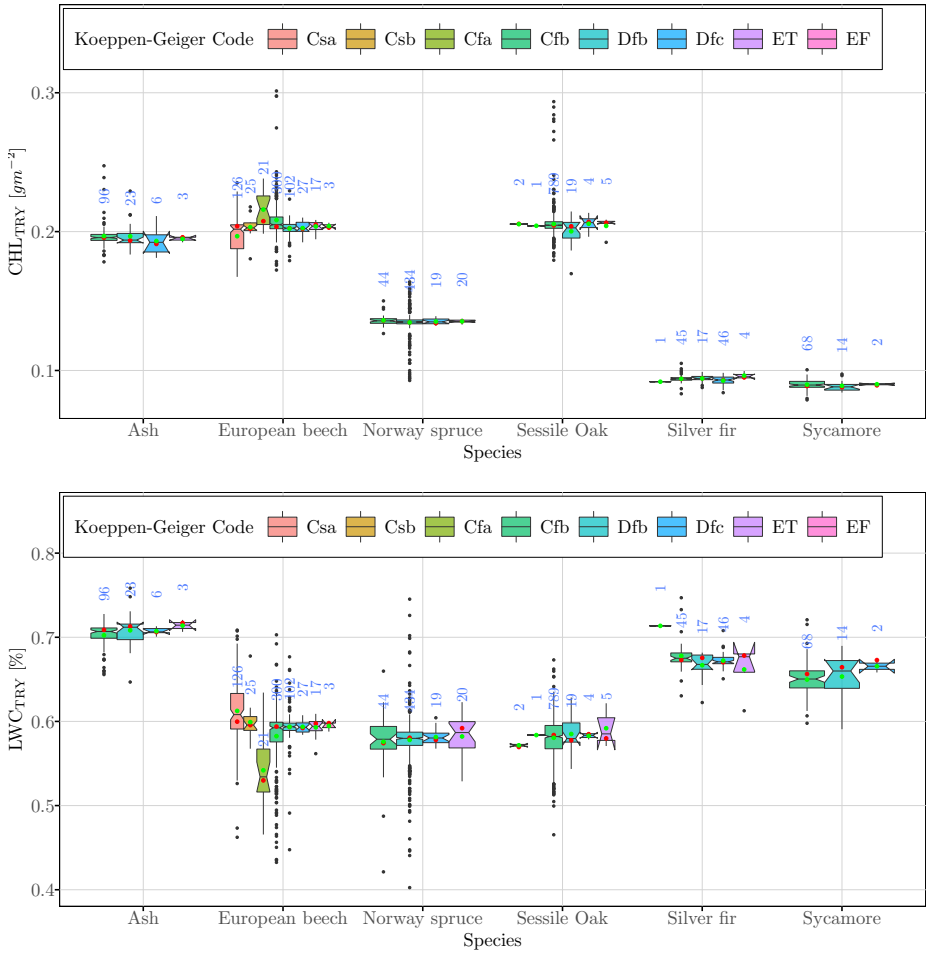

Figure 13: The Figures show the ranges of CHL_{TRY} and LWC_{TRY} in different climatic regions after Köppen-Geiger climate classification (Peel et al., 2007). The notches, indicating if the medians differ with 95% confidence, show that the median values are relatively stable. The mode (●), however, is more stable than the median and the mean (●) across different climate zones and species. The number of samples are annotated in blue.

F | Relative traits, Lägern vs subplot P1

The extrapolation of the species to the Lägern site is a critical step. The larger area is expected to have a larger variation than subplot subplot P1. Figure 14 shows the differences of the traits between Lägern and P1. The height distribution differes significantly as the plot P1 consists of old, full-grown trees. The Lägern is vegetated by young, smaller trees, though. It turns out that the variations across the larger area is very similar to P1 for the canopy traits. This can be interpreted in two ways: Either, the trait variation is represented in the smaller area. This means that the trait variations are less dependent on environmental factors like slope, exposure, soil etc. Following this logic, the composition of small patches is representative for a larger area. Another interpretation is that the measurement via VIs is more dependent on the disturbing factors like canopy structure, the trait signal disappears in the noise. It is likely that a mixture of both explanatory approaches persists.

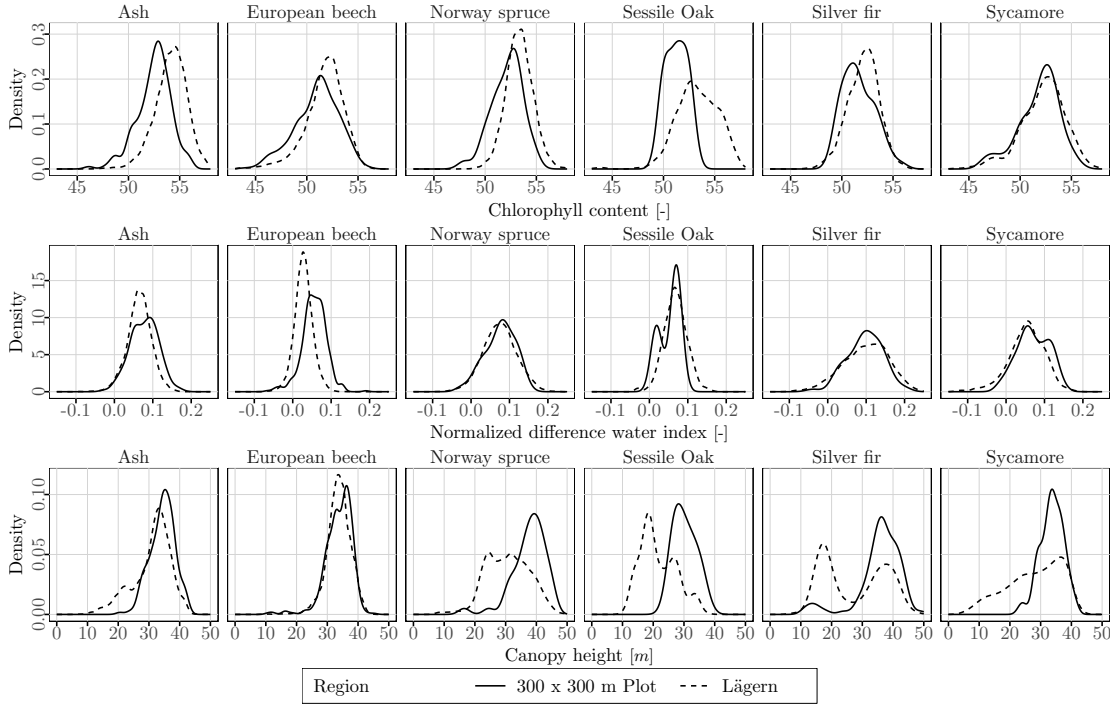

Figure 14: The VI densities shown for Lägern and the subplot P1 are very similar. Only the height distribution differs strongly. This is due to the fact that the subplot P1 is populated by full-grown trees.

G | LAI map of Lägern

LAI_{APEX} 15 was derived for post-processing of the VIs CHL_{APEX} and LWC_{APEX}. Pixels with an $LAI_{APEX}<2$ were removed as being considered as non-dense or non-vegetation.

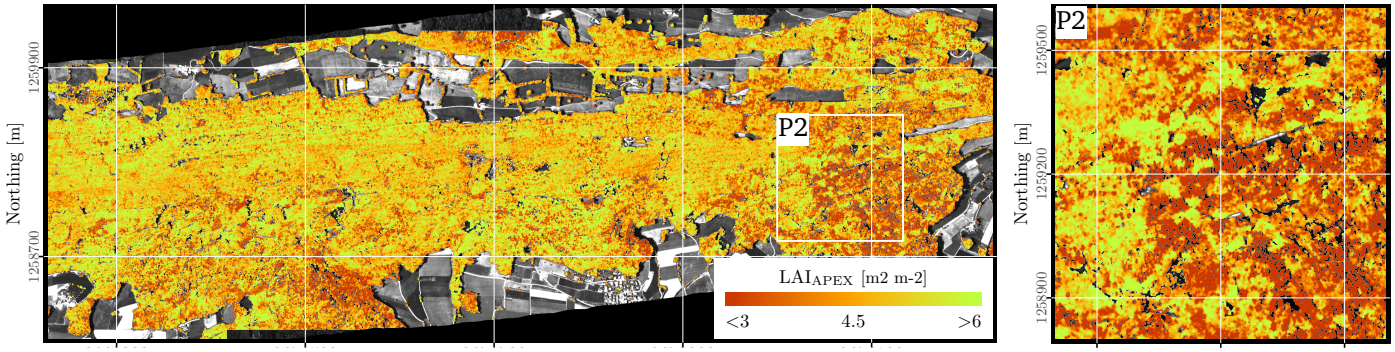

Figure 15: LAI_{APEX} of Lägern, derived from APEX multispectral data after correction for shadowing effects. The values vary strongly between coniferous and deciduous species (see species classification Figure 5). The subplot on the righthand side shows the close-up view of plot P2. The shadow effect correction performed well for LAI_{APEX}.

H | Interpolation of CHL_{TRY} and LWC_{TRY}

The trait data covering Europe has been used to test a simple spatial interpolation approach. All species (Table 2) present in the gap-filled TRY database at hand have been used (which is a small subset of the vast amount of species present in the raw TRY dataset). The spatial distribution and the density of the data-points is displayed in Fig. 17.

The method used here is an admittedly simplistic approach. The idea was to perform regression Kriging (Pebesma, 2006) using climatology and soil data as predictors. This includes first performing a regression and then applying Kriging on the residuals. The regression was was done using random forests (RF, Liaw & Wiener (2002)).

Table 2: The table shows the tree species that have been used for trait interpolation. The number of samples per species are displayed.

Species name	Species type	Number of observations
Abies alba	conifer	113
Acer campestre	deciduous	27
Acer platanoides	deciduous	53
Acer pseudoplatanus	deciduous	84
Carpinus betulus	deciduous	60
Fagus sylvatica	deciduous	621
Fraxinus excelsior	deciduous	128
Picea abies	conifer	517
Pinus sylvestris	conifer	1875
Quercus petraea	deciduous	820
Sorbus aria	deciduous	62
Tilia platyphyllos	deciduous	12
Ulmus glabra	deciduous	86
Total	—	4458

Soil data was extracted from the harmonized world soil database (HWSD) version 1.2 (Wieder (2014); `http://www.iiasa.ac.at/Research/LUC/External-World-soil-database/HTML`) and climate data is obtained from WorldClim – Global Climate Data Version 1.4 (Hijmans et al. (2005); `http://www.worldclim.org/`). The soil dataset was resampled using nearest neighbor interpolation from a resolution of 0.05° to the WorldClim data, which has a resolution of approximately 0.008° (∼1 km). A principal component analysis (PCA) was performed and the first five

components for each dataset (shown in Fig. 16) were extracted for the TRY data-points.

The random forest (RF) model was trained for CHL_{TRY} and LWC_{TRY} with the principle components, longitude and latitude as predictors using 10-fold cross validation. For CHL_{TRY}, root-mean-square error (RMSE) was 0.028 ± 0.002 and R^2 was 0.642 ± 0.036. LWC_{TRY} performed worse with RMSE 0.031 ± 0.002 and R^2 0.476 ± 0.067. These results have to be regarded with caution, as discussed later. For both traits, climate variables, latitude and longitude are more important than soil. This is shown in the variable importance plot, Figure 18.

The model was then used to interpolate the traits across Europe. The resulting prediction maps are shown in Figure 17. The residuals of the prediction do not show any spatial dependency structure for both variables CHL_{TRY} and LWC_{TRY}, which becomes apparent when checking the variograms (Fig. 19). Thus, no Kriging is done on the residuals.

Additionally, species-wise modeling using RF regression has been tested. The prediction maps for Europe for CHL_{TRY} and LWC_{TRY} are shown in Fig. 20 and 21 respectively, together with the mean R^2 and its standard deviation over 10-fold cross-validation. For the most species, the models perform bad (low R^2 and high variation of the performance). Some species (e.g. *Fagus sylvatica* and *Picea abies*) show a decent performance.

Both interpolation approaches, all species in combination and single species, have to be viewed with skepticism. First, the sampling is not randomized. Some sampled species are highly concentrated to certain sites, which can lead to an overestimation of the model accuracy. Sessile oak, for example, has been sampled hundreds of times in West France at a single site. The interpolation might work well for these individuals which have, through their superior number, more weight than other individuals at sites with less samples. Second, the species are not distributed randomly, they are more likely to appear at places that are more suitable in terms of environmental conditions. Thus, an interpolation to sites where the species does not find good environmental conditions may yield unrealistic trait values. These problems could be solved statistically by weighting of the performance metrics or including species distribution maps, for example. Of course, more sophisticated models and inclusion of more diverse environmental data (e.g. satellite data) must be considered to achieve better results.

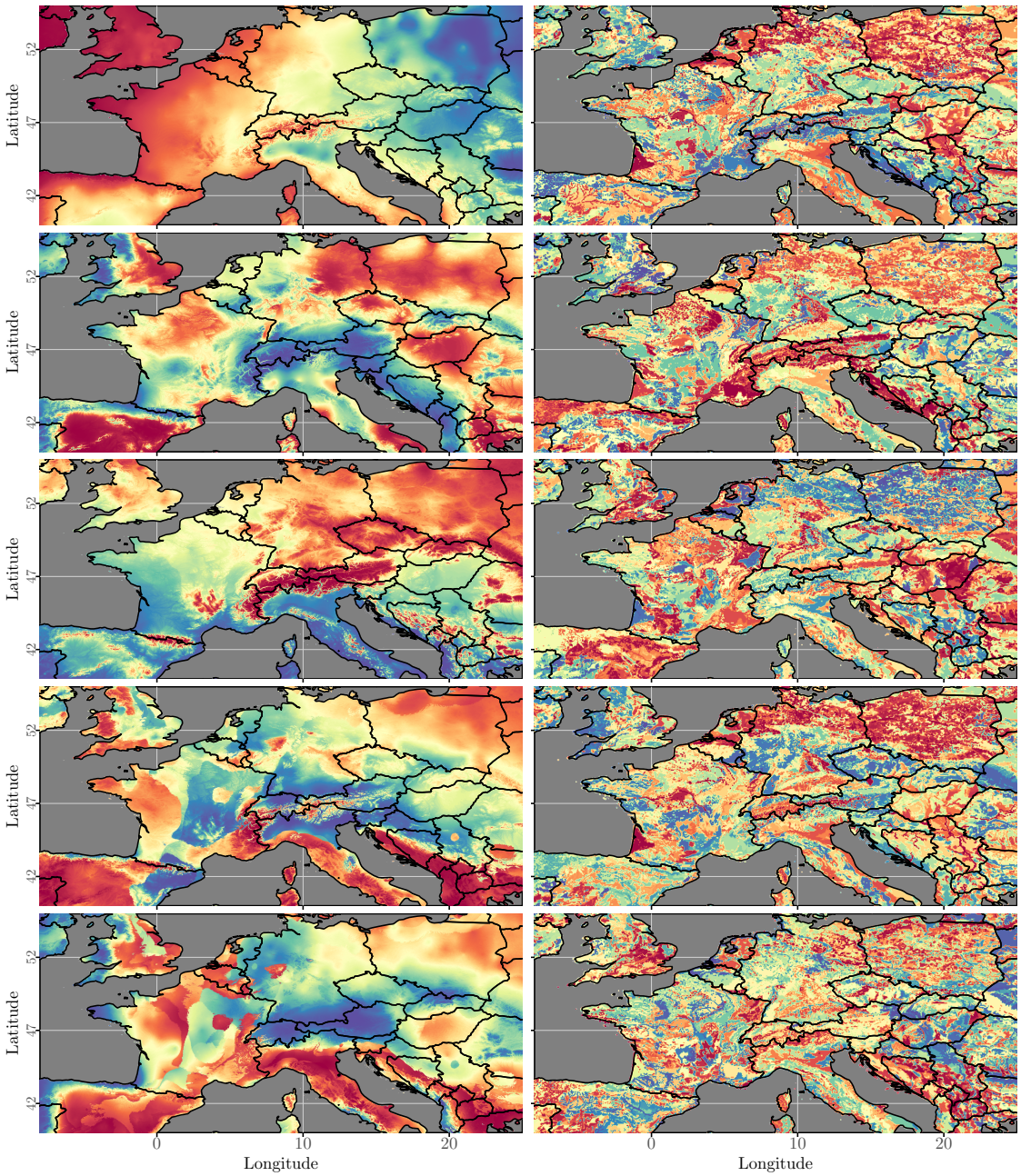

Figure 16: First five principle components of WorldClim (left column) and HWSD (right column) data. The first principle components are on the top line, the last on the bottom. The data has been used as predictors for CHL_{TRY} and LWC_{TRY} interpolation. Histogram equalization has been applied to the maps to enhance the contrast for better visualization.

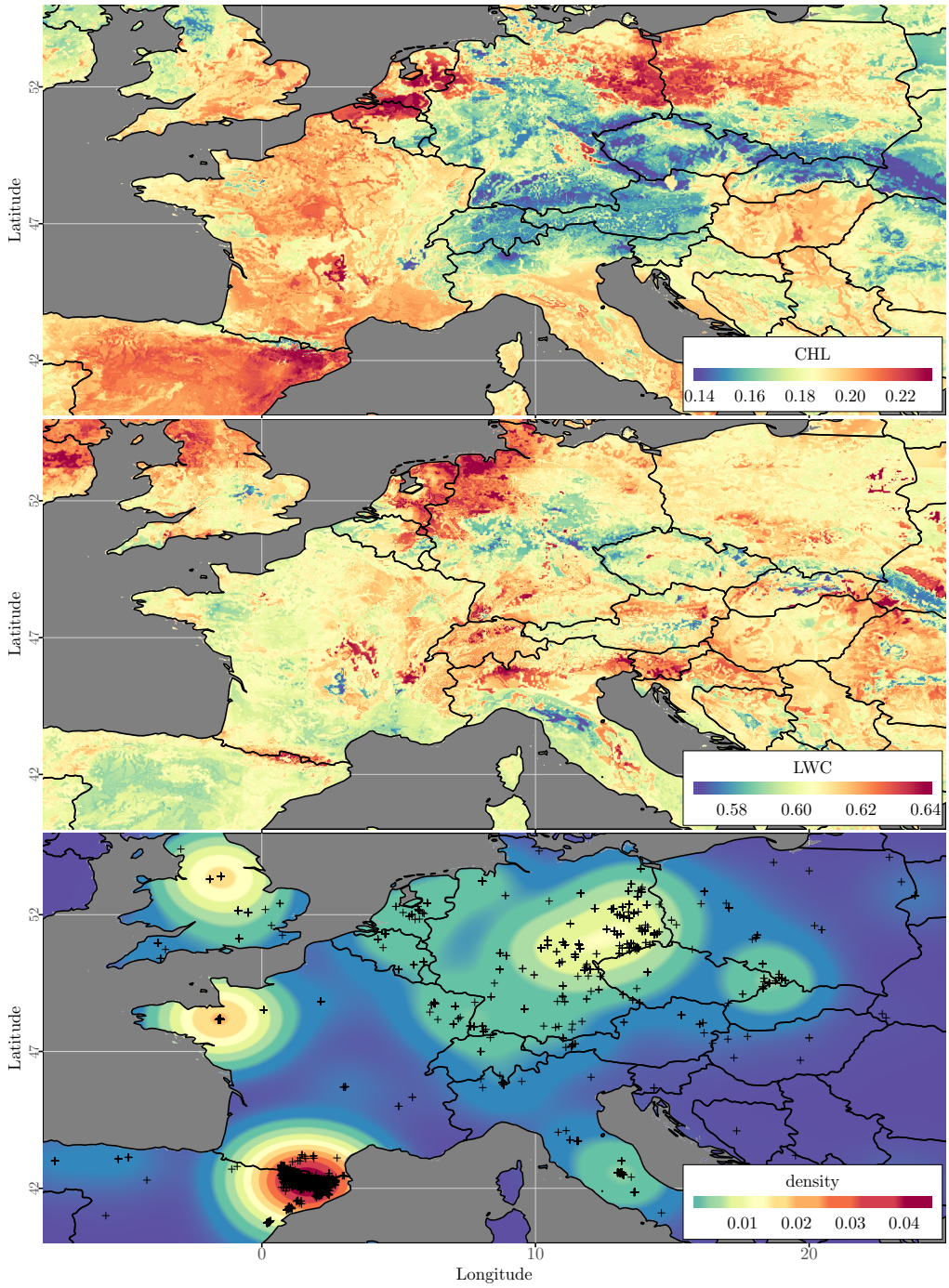

Figure 17: The Figures show the TRY traits interpolation for Europe with CHL_{TRY} on top, LWC_{TRY} in the middle and the sample density in the bottom plot. The interpolation was done using RF regression for all species (shown in Table 2) together.

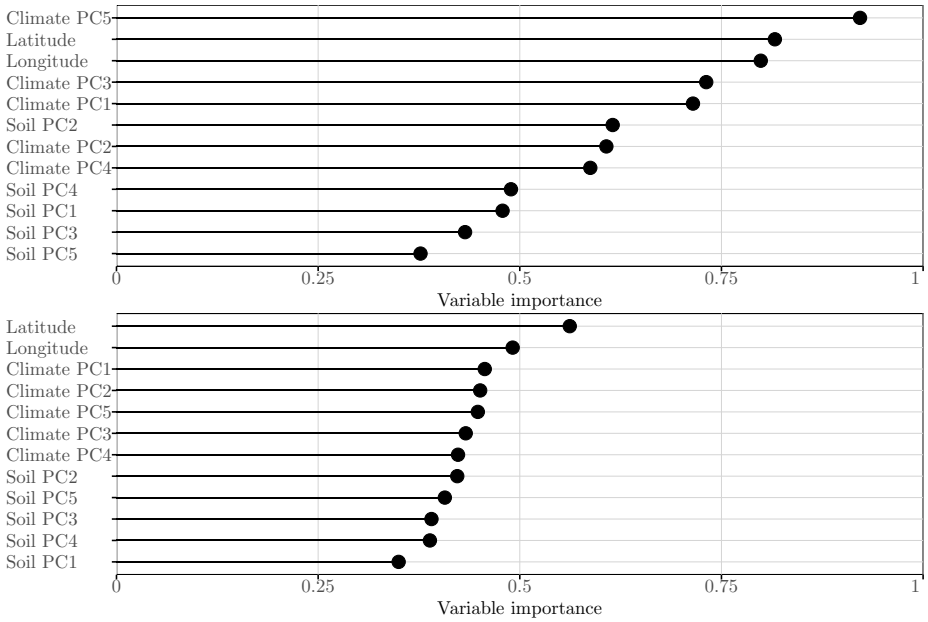

Figure 18: The Figures show the importance of the variables used in the RF regression for CHL_{TRY} (top) and LWC_{TRY} (bottom). In both cases, climate, latitude and longitude are more important than the soil properties.

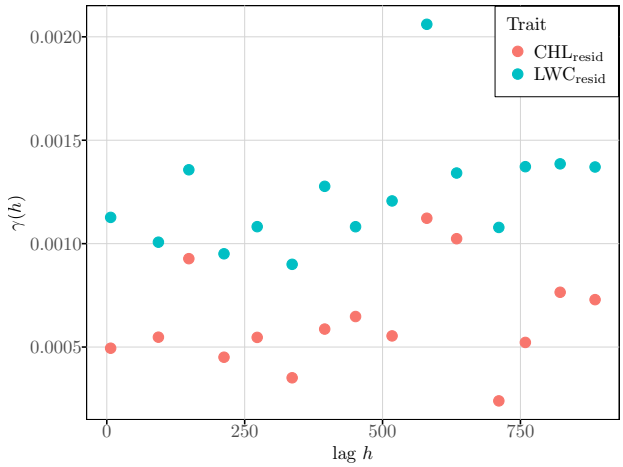

Figure 19: The figure shows the variograms of the residuals of the traits CHL and LWC. The model was fitted using random forest. The residuals do not show any lag dependency, indicating that they are spatially random.

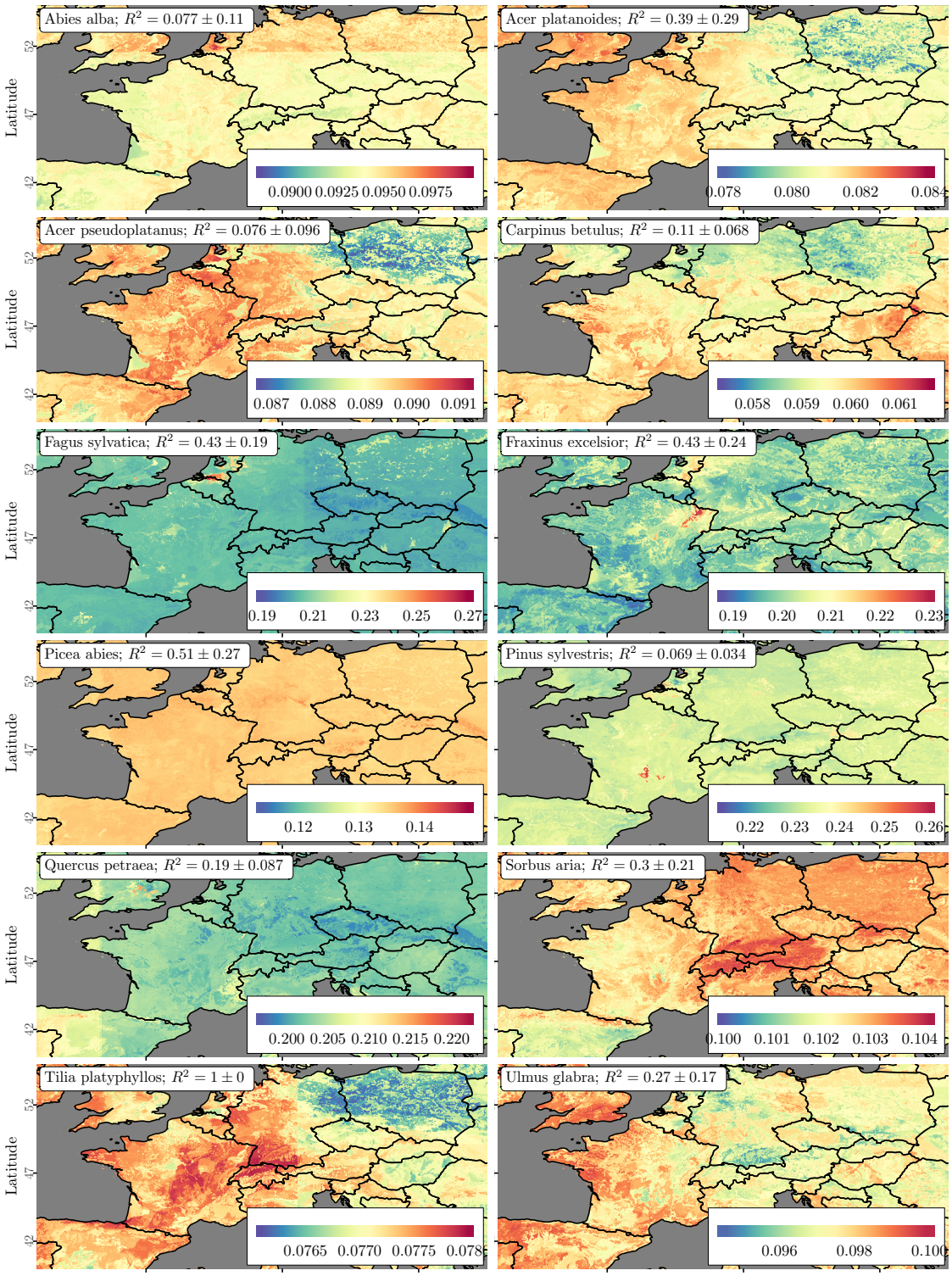

Figure 20: Species-wise trait interpolation of CHL_{TRY}. The color ranges cannot be compared across the plots. The interpolation has been done using RF regression, the R^2 is displayed for each species. For some species, the model performs very badly, the variation of R^2 across the 10-fold cross validation (reported as $\pm$ sd) is large in the most cases, especially if the number of samples is small. Some species (e.g. *Fagus sylvatica* and *Picea abies*) perform quite well, which might be related to the larger number of samples. *Tilia platyphyllow*, has a reported R^2 of 1, which is wrong. The cause is that only 12 samples are present, which causes the cross-validation to report this unrealistic value.

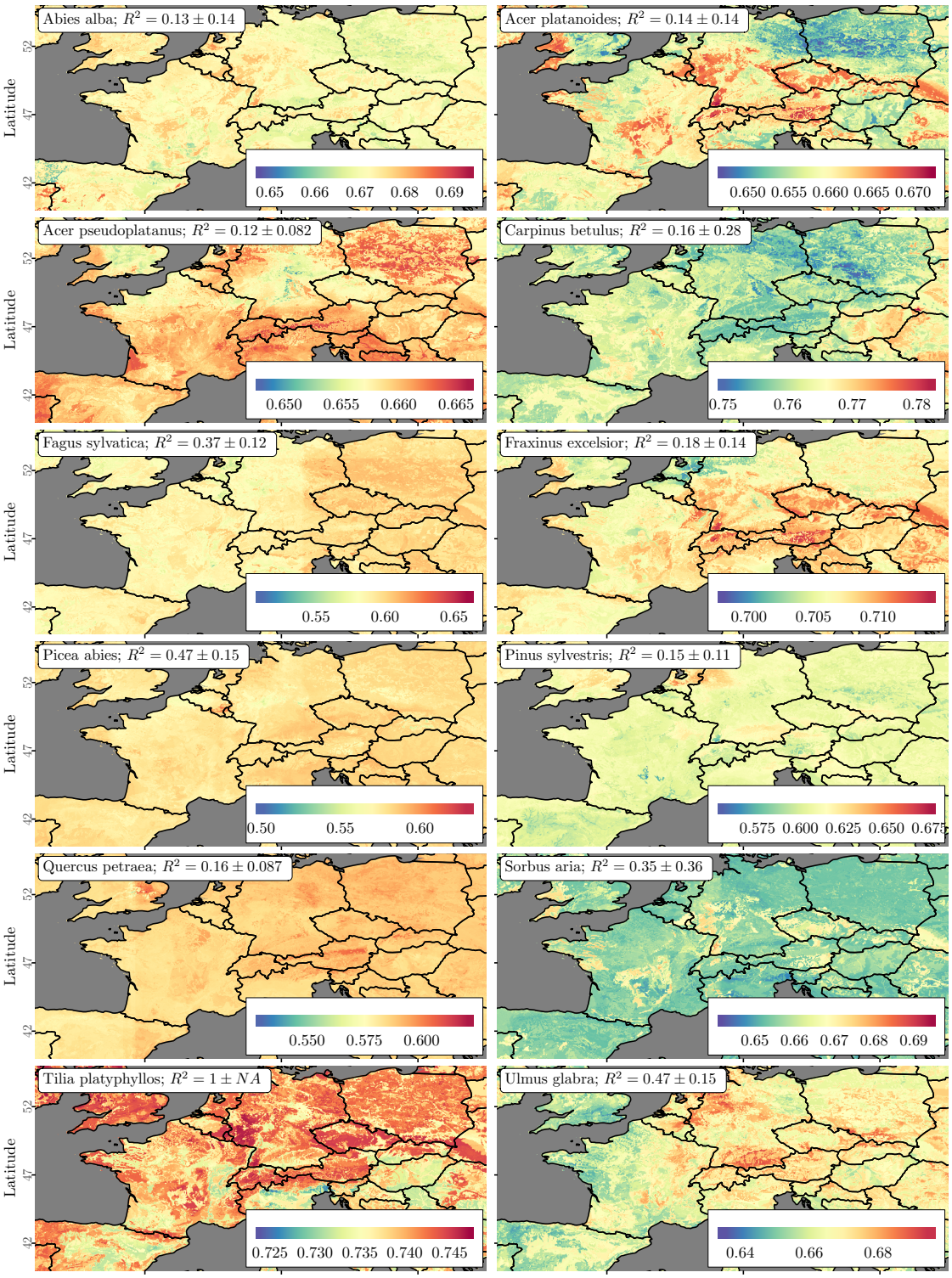

Figure 21: Species-wise trait interpolation of LWC_{TRY}. The color ranges cannot be compared across the plots. The interpolation has been done using RF regression, the R^2 is displayed for each species. For the most species, the model performs very badly, the variation of R^2 across the 10-fold cross validation (reported as $\pm$ sd) is large in the most cases, especially if the number of samples is small. Some species (*Fagus sylvatica*, *Picea abies* and *Ulmus glabra*) perform well, which might be related to the larger number of samples. *Tilia platyphyllow*, has a reported R^2 of 1, which is wrong. The cause is that only 12 samples are present, which causes the cross-validation to report this unrealistic value.

References

Asner, G. P., & Martin, R. E. (2016). Spectranomics: Emerging science and conservation opportunities at the interface of biodiversity and remote sensing. *Global Ecology and Conservation*, *8*, 212–219.

Asner, G. P., Martin, R. E., Anderson, C. B., & Knapp, D. E. (2015). Quantifying forest canopy traits: Imaging spectroscopy versus field survey. *Remote Sensing of Environment*, *158*, 15–27.

de Bello, F., Lavorel, S., Díaz, S., Harrington, R., Cornelissen, J. H., Bardgett, R. D., Berg, M. P., Cipriotti, P., Feld, C. K., Hering, D. et al. (2010). Towards an assessment of multiple ecosystem processes and services via functional traits. *Biodiversity and Conservation*, *19*, 2873–2893.

Blackburn, G. A. (2007). Hyperspectral remote sensing of plant pigments. *Journal of experimental botany*, *58*, 855–867.

van Bodegom, P. M., Douma, J. C., & Verheijen, L. M. (2014). A fully traits-based approach to modeling global vegetation distribution. *Proceedings of the National Academy of Sciences*, *111*, 13733–13738.

van Bodegom, P. M., Douma, J. C., Witte, J. P. M., Ordoñez, J. C., Bartholomeus, R. P., & Aerts, R. (2012). Going beyond limitations of plant functional types when predicting global ecosystem–atmosphere fluxes: exploring the merits of traits-based approaches. *Global Ecology and Biogeography*, *21*, 625–636.

Cadotte, M. W., Carscadden, K., & Mirotchnick, N. (2011). Beyond species: functional diversity and the maintenance of ecological processes and services. *Journal of Applied Ecology*, *48*, 1079–1087.

Cardinale, B. J., Duffy, J. E., Gonzalez, A., Hooper, D. U., Perrings, C., Venail, P., Narwani, A., Mace, G. M., Tilman, D., Wardle, D. A. et al. (2012). Biodiversity loss and its impact on humanity. *Nature*, *486*, 59–67.

Chang, C.-C., & Lin, C.-J. (2011). Libsvm: a library for support vector machines. *ACM Transactions on Intelligent Systems and Technology (TIST)*, *2*, 27.

Cohen, J. (1960). A coefficient of agreement for nominal scale. *Educational and Psychological Measurement*, *20*, 37–46.

Cornelissen, J., Lavorel, S., Garnier, E., Diaz, S., Buchmann, N., Gurvich, D., Reich, P., Ter Steege, H., Morgan, H., Van Der Heijden, M. et al. (2003). A handbook of protocols for standardised and easy measurement of plant functional traits worldwide. *Australian journal of Botany*, *51*, 335–380.

Costanza, R., d'Arge, R., De Groot, R., Faber, S., Grasso, M., Hannon, B., Limburg, K., Naeem, S., O'neill, R. V., Paruelo, J. et al. (1997). The value of the world's ecosystem services and natural capital, .

Crutzen, P. J. (2006). The "anthropocene". In *Earth system science in the anthropocene* (pp. 13–18). Springer.

Damm, A., Guanter, L., Verhoef, W., Schläpfer, D., Garbari, S., & Schaepman, M. (2015). Impact of varying irradiance on vegetation indices and chlorophyll fluorescence derived from spectroscopy data. *Remote Sensing of Environment*, *156*, 202–215.

Demir, B., & Ertrk, S. (2009). Improving SVM classification accuracy using a hierarchical approach for hyperspectral images. In *2009 16th IEEE International Conference on Image Processing ICIP 2009* (pp. 2849–2852). IEEE.

Díaz, S., & Cabido, M. (2001). Vive la différence: plant functional diversity matters to ecosystem processes. *TRENDS in Ecology & Evolution*, *16*.

Díaz, S., Kattge, J., Cornelissen, J. H., Wright, I. J., Lavorel, S., Dray, S., Reu, B., Kleyer, M., Wirth, C., Prentice, I. C. et al. (2016). The global spectrum of plant form and function. *Nature*, *529*, 167–171.

Díaz, S., Lavorel, S., de Bello, F., Quétier, F., Grigulis, K., & Robson, T. M. (2007). Incorporating plant functional diversity effects in ecosystem service assessments. *Proceedings of the National Academy of Sciences*, *104*, 20684–20689.

Eugster, W., Zeyer, K., Zeeman, M., Michna, P., Zingg, A., Buchmann, N., & Emmenegger, L. (2007). Methodical study of nitrous oxide eddy covariance measurements using quantum cascade laser spectrometery over a swiss forest. *Biogeosciences*, *4*, 927–939.

Exelis Visual Information Solutions (2015). Envi v5.3.

Feilhauer, H., Doktor, D., Schmidtlein, S., & Skidmore, A. K. (2016). Mapping pollination types with remote sensing. *Journal of Vegetation Science*, *27*, 999–1011.

Féret, J.-B., & Asner, G. P. (2013). Tree species discrimination in tropical forests using airborne imaging spectroscopy. *IEEE Transactions on Geoscience and Remote Sensing*, *51*, 73–84.

Friedl, M. A., McIver, D. K., Hodges, J. C., Zhang, X., Muchoney, D., Strahler, A. H., Woodcock, C. E., Gopal, S., Schneider, A., Cooper, A. et al. (2002). Global land cover mapping from modis: algorithms and early results. *Remote Sensing of Environment*, *83*, 287–302.

Gao, B.-C. (1996). Ndwi—a normalized difference water index for remote sensing of vegetation liquid water from space. *Remote sensing of environment*, *58*, 257–266.

Garbulsky, M. F., Filella, I., & Peñuelas, J. (2013). Recent advances in the estimation of photosynthetic stress for terrestrial ecosystem services related to carbon uptake. *Earth Observation of Ecosystem Services*, (p. 39).

Grimm, B. (2001). Chlorophyll: Structure and function. *eLS*, .

Heiskanen, J. (2006). Estimating aboveground tree biomass and leaf area index in a mountain birch forest using aster satellite data. *International Journal of Remote Sensing*, *27*, 1135–1158.

Hijmans, R. J., Cameron, S. E., Parra, J. L., Jones, P. G., & Jarvis, A. (2005). Very high resolution interpolated climate surfaces for global land areas. *International journal of climatology*, *25*, 1965–1978.

Hilker, T., van Leeuwen, M., Coops, N. C., Wulder, M. A., Newnham, G. J., Jupp, D. L., & Culvenor, D. S. (2010). Comparing canopy metrics derived from terrestrial and airborne laser scanning in a douglas-fir dominated forest stand. *Trees*, *24*, 819–832.

Homolova, L., Malenovskỳ, Z., Clevers, J. G., García-Santos, G., & Schaepman, M. E. (2013). Review of optical-based remote sensing for plant trait mapping. *Ecological Complexity*, *15*, 1–16.

Hueni, A., Lenhard, K., Baumgartner, A., & Schaepman, M. E. (2013). Airborne prism experiment calibration information system. *IEEE Transactions on Geoscience and Remote Sensing*, *51*, 5169–5180.

IPCC (2014). *Climate Change 2014: Synthesis Report. Contribution of Working Groups I, II and III to the Fifth Assessment Report of the Intergovernmental Panel on Climate Change [Core Writing Team, R.K. Pachauri and L.A. Meyer (eds.)]*. IPCC.

Jetz, W., Cavender-Bares, J., Pavlick, R., Schimel, D., Davis, F. W., Asner, G. P., Guralnick, R., Kattge, J., Latimer, A. M., Moorcroft, P. et al. (2016). Monitoring plant functional diversity from space. *Nature plants*, *2*, 16024.

Jetz, W., McPherson, J. M., & Guralnick, R. P. (2012). Integrating biodiversity distribution knowledge: toward a global map of life. *Trends in ecology & evolution*, *27*, 151–159.

de Jong, R., Verbesselt, J., Zeileis, A., & Schaepman, M. E. (2013). Shifts in global vegetation activity trends. *Remote Sensing*, *5*, 1117–1133.

Kattge, J., Díaz, S., Lavorel, S., Prentice, I. C., Leadley, P., Bönisch, G., Garnier, E., Westoby, M., Reich, P. B., Wright, I. J., Cornelissen, J. H. C., Violle, C., Harrison, S. P., Van Bodegom, P. M., Reichstein, M., J, E. B., Soudzilovskaia, N. A., Ackerly, D. D., Anand, M., Atkin, O., Bahn, M., Baker, T. R., Baldocchi, D., Bekker, R., Blanco, C. C., Blonder, B., Bond, W. J., Bradstock, R., Bunker, D. E., Casanoves, F., Cavender Bares, J., Chambers, J. Q., Chapin III, F. S., Chave, J., Coomes, D., Cornwell, W. K., Craine, J. M., Dobrin, B. H., Duarte, L., Durka, W., Elser, J., Esser, G., Estiarte, M., Fagan, W. F., Fang, J., Fernández Méndez, F., Fidelis, A., Finegan, B., Flores, O., Ford, H., Frank, D., Freschet, G. T., Fyllas, N. M., Gallagher, R. V., Green, W. A., Gutierrez, A. G., Hickler, T., Higgins, S. I., Hodgson, J. G., Jalili, A., Jansen, S., Joly, C. A., Kerkhoff, A. J., Kirkup, D., Kitajima, K., Kleyer, M., Klotz, S., Knops, J. M. H., Kramer, K., Kühn, I., Kurokawa, H., Laughlin, D., Lee, T. D., Leishman, M., Lens, F., Lenz, T., Lewis, S. L., Lloyd, J., Llusià, J., Louault, F., MA, S., Mahecha, M. D., Manning, P., Massad, T., Medlyn, B. E., Messier, J., Moles, A. T., Müller, S. C., Nardowski, K., Naeem, S., Niinemets, Ü., Nöllert, S., Nüske, A., Ogaya, R., Oleskyn, J., Onipchenko, V. G., Onoda, Y., Ordoñes, J., Overbeck, G. et al. (2011). TRY – a global database of plant traits. *Global Change Biology*, *17*, 2905–2935.

Kokaly, R. F., Asner, G. P., Ollinger, S. V., Martin, M. E., & Wessman, C. A. (2009). Characterizing canopy biochemistry from imaging spectroscopy and its application to ecosystem studies. *Remote Sensing of Environment*, *113*, S78–S91.

Lausch, A., Bannehr, L., Beckmann, M., Boehm, C., Feilhauer, H., Hacker, J., Heurich, M., Jung, A., Klenke, R., Neumann, C. et al. (2016). Linking earth observation and taxonomic, structural and functional biodiversity: Local to ecosystem perspectives. *Ecological Indicators*, *70*, 317–339.

Lavorel, S., Diaz, S., Cornelissen, J. H. C., Garnier, E., Harrison, S. P., McIntyre, S., Pausas, J. G., Pérez-Harguindeguy, N., Roumet, C., & Urcelay, C. (2007). Plant Functional Types: Are We Getting Any Closer to the Holy Grail? In *Terrestrial Ecosystems in a Changing World* (pp. 149–164). Berlin, Heidelberg: Springer Berlin Heidelberg.

van Leeuwen, M., & Nieuwenhuis, M. (2010). Retrieval of forest structural parameters using lidar remote sensing. *European Journal of Forest Research*, *129*, 749–770.

Lewis, S. L., & Maslin, M. A. (2015). Geological evidence for the anthropocene. *Science*, *349*, 246–247.

Liaw, A., & Wiener, M. (2002). Classification and regression by randomforest. *R news*, *2*, 18–22.

Lillesand, T. M., Kiefer, R. W., Chipman, J. W. et al. (2008). *Remote sensing and image interpretation.*. (6th ed.). John Wiley & Sons Ltd.

Lindenmayer, D., & Likens, G. E. (2013). Benchmarking open access science against good science. *The Bulletin of the Ecological Society of America*, *94*, 338–340.

Malenovský, Z., Homolová, L., Zurita-Milla, R., Lukeš, P., Kaplan, V., Hanuš, J., Gastellu-Etchegorry, J.-P., & Schaepman, M. E. (2013). Retrieval of spruce leaf chlorophyll content from airborne image data using continuum removal and radiative transfer. *Remote Sensing of Environment*, *131*, 85–102.

Martin, M., Newman, S., Aber, J., & Congalton, R. (1998). Determining forest species composition using high spectral resolution remote sensing data. *Remote Sensing of Environment*, *65*, 249–254.

Marvin, D. C., Asner, G. P., Knapp, D. E., Anderson, C. B., Martin, R. E., Sinca, F., & Tupayachi, R. (2014). Amazonian landscapes and the bias in field studies of forest structure and biomass. *Proceedings of the National Academy of Sciences*, *111*, E5224–E5232.

McGill, B. J., Enquist, B. J., Weiher, E., & Westoby, M. (2006). Rebuilding community ecology from functional traits. *Trends in ecology & evolution*, *21*, 178–185.

Meehl, G. A., Stocker, T. F., Collins, W. D., Friedlingstein, P., Gaye, A. T., Gregory, J. M., Kitoh, A., Knutti, R., Murphy, J. M., Noda, A. et al. (2007). Global climate projections. *Climate change*, *3495*, 747–845.

Melgani, F., & Bruzzone, L. (2004). Classification of hyperspectral remote sensing images with support vector machines. *IEEE Transactions on geoscience and remote sensing*, *42*, 1778–1790.

Meyer, D., Dimitriadou, E., Hornik, K., & Weingessel, A. (2015). e1071: Misc Functions of the Department of Statistics, Probability Theory Group (Formerly: E1071), TU Wien.

Mountrakis, G., Im, J., & Ogole, C. (2011). Support vector machines in remote sensing: A review. *ISPRS Journal of Photogrammetry and Remote Sensing*, *66*, 247–259.

Pebesma, E. J. (2006). The role of external variables and gis databases in geostatistical analysis. *Transactions in GIS*, *10*, 615–632.

Peel, M. C., Finlayson, B. L., & McMahon, T. A. (2007). Updated world map of the köppen-geiger climate classification. *Hydrology and earth system sciences discussions*, *4*, 439–473.

Petchey, O. L., & Gaston, K. J. (2006). Functional diversity: back to basics and looking forward. *Ecology letters*, *9*, 741–758.

Pettorelli, N., Wegmann, M., Skidmore, A., Mücher, S., Dawson, T. P., Fernandez, M., Lucas, R., Schaepman, M. E., Wang, T., O'Connor, B. et al. (2016). Framing the concept of satellite remote sensing essential biodiversity variables: challenges and future directions. *Remote Sensing in Ecology and Conservation*, .

Pigliucci, M. (2001). *Phenotypic plasticity: beyond nature and nurture*. The John Hopkins University Press.

Richter, R., & Schläpfer, D. (2002). Geo-atmospheric processing of airborne imaging spectrometry data. part 2: atmospheric/topographic correction. *International Journal of Remote Sensing*, *23*, 2631–2649.

Sala, O. E., Chapin, F. S., Armesto, J. J., Berlow, E., Bloomfield, J., Dirzo, R., Huber-Sanwald, E., Huenneke, L. F., Jackson, R. B., Kinzig, A. et al. (2000). Global biodiversity scenarios for the year 2100. *science*, *287*, 1770–1774.

Schaepman, M. E., Jehle, M., Hueni, A., D'Odorico, P., Damm, A., Weyermann, J., Schneider, F. D., Laurent, V., Popp, C., Seidel, F. C. et al. (2015). Advanced radiometry measurements and earth science applications with the airborne prism experiment (apex). *Remote Sensing of Environment*, *158*, 207–219.

Schaepman, M. E., Ustin, S. L., Plaza, A. J., Painter, T. H., Verrelst, J., & Liang, S. (2009). Earth system science related imaging spectroscopy—an assessment. *Remote Sensing of Environment*, *113*, S123–S137.

Scheiter, S., Langan, L., & Higgins, S. I. (2013). Next-generation dynamic global vegetation models: learning from community ecology. *New Phytologist*, *198*, 957–969.

Schimel, D., Pavlick, R., Fisher, J. B., Asner, G. P., Saatchi, S., Townsend, P., Miller, C., Frankenberg, C., Hibbard, K., & Cox, P. (2015). Observing terrestrial ecosystems and the carbon cycle from space. *Global change biology*, *21*, 1762–1776.

Schläpfer, D., & Richter, R. (2002). Geo-atmospheric processing of airborne imaging spectrometry data. part 1: parametric orthorectification. *International Journal of Remote Sensing*, *23*, 2609–2630.

Schneider, F. D., Leiterer, R., Morsdorf, F., Gastellu-Etchegorry, J.-P., Lauret, N., Pfeifer, N., & Schaepman, M. E. (2014). Simulating imaging spectrometer data: 3d forest modeling based on lidar and in situ data. *Remote Sensing of Environment*, *152*, 235–250.

Schneider, F. D., Leiterer, R., Schaepman, M. E., & Morsdorf, F. (2015). Canopy height and plant area index changes in a temperate forest between 2010–2014 using airborne laser scanning. In *SilviLaser Conference, La Grande Motte, France, 28 September 2015 - 30 September 2015* (pp. 156–158).

Schrodt, F., Kattge, J., Shan, H., Fazayeli, F., Joswig, J., Banerjee, A., Reichstein, M., Bönisch, G., Díaz, S., Dickie, J. et al. (2015). Bhpmf–a hierarchical bayesian approach to gap-filling and trait prediction for macroecology and functional biogeography. *Global Ecology and Biogeography*, *24*, 1510–1521.

Secretariat of the Convention on Biological Diversity (2005). *Handbook of the convention on biological diversity* volume 3. London: Earthscan.

Shan, H., Kattge, J., Reich, P., Banerjee, A., Schrodt, F., & Reichstein, M. (2012). Gap filling in the plant kingdom—trait prediction using hierarchical probabilistic matrix factorization. In *Proceedings of the 29th International Conference on Machine Learning (ICML-12)* (pp. 1303–1310).

Skidmore, A. K., & Pettorelli, N. (2015). Agree on biodiversity metrics to track from space: ecologists and space agencies must forge a global monitoring strategy. *Nature*, *523*, 403–406.

Steffen, W., Crutzen, P. J., & McNeill, J. R. (2007). The anthropocene: are humans now overwhelming the great forces of nature. *AMBIO: A Journal of the Human Environment*, *36*, 614–621.

Steffen, W., Sanderson, R. A., Tyson, P. D., Jäger, J., Matson, P. A., Moore III, B., Oldfield, F., Richardson, K., Schellnhuber, H. J., Turner, B. L. et al. (2004). *Global change and the earth system: a planet under pressure*. Springer Science & Business Media.

Stimson, H. C., Breshears, D. D., Ustin, S. L., & Kefauver, S. C. (2005). Spectral sensing of foliar water conditions in two co-occurring conifer species: Pinus edulis and juniperus monosperma. *Remote Sensing of Environment*, *96*, 108–118.

Swenson, N. G. (2014). Phylogenetic imputation of plant functional trait databases. *Ecography*, *37*, 105–110.

Tittensor, D. P., Walpole, M., Hill, S. L., Boyce, D. G., Britten, G. L., Burgess, N. D., Butchart, S. H., Leadley, P. W., Regan, E. C., Alkemade, R. et al. (2014). A mid-term analysis of progress toward international biodiversity targets. *Science*, *346*, 241–244.

Tucker, C., & Townshend, J. R. (2000). Strategies for monitoring tropical deforestation using satellite data. *International Journal of Remote Sensing*, *21*, 1461–1471.

Turner, W., Rondinini, C., Pettorelli, N., Mora, B., Leidner, A. K., Szantoi, Z., Buchanan, G., Dech, S., Dwyer, J., Herold, M. et al. (2015). Free and open-access satellite data are key to biodiversity conservation. *Biological Conservation*, *182*, 173–176.

Turner, W., Spector, S., Gardiner, N., Fladeland, M., Sterling, E., & Steininger, M. (2003). Remote sensing for biodiversity science and conservation. *Trends in ecology & evolution*, *18*, 306–314.

Ustin, S. L., Gitelson, A. A., Jacquemoud, S., Schaepman, M., Asner, G. P., Gamon, J. A., & Zarco-Tejada, P. (2009). Retrieval of foliar information about plant pigment systems from high resolution spectroscopy. *Remote Sensing of Environment*, *113*, S67–S77.

Ustin, S. L., Roberts, D. A., Gamon, J. A., Asner, G. P., & Green, R. O. (2004). Using imaging spectroscopy to study ecosystem processes and properties. *BioScience*, *54*, 523–534.

Violle, C., Enquist, B. J., McGill, B. J., Jiang, L., Albert, C. H., Hulshof, C., Jung, V., & Messier, J. (2012). The return of the variance: intraspecific variability in community ecology. *Trends in ecology & evolution*, *27*, 244–252.

Violle, C., Navas, M.-L., Vile, D., Kazakou, E., Fortunel, C., Hummel, I., & Garnier, E. (2007). Let the concept of trait be functional! *Oikos*, *116*, 882–892.

Violle, C., Reich, P. B., Pacala, S. W., Enquist, B. J., & Kattge, J. (2014). The emergence and promise of functional biogeography. *Proceedings of the National Academy of Sciences*, *111*, 13690–13696.

Waters, C. N., Zalasiewicz, J., Summerhayes, C., Barnosky, A. D., Poirier, C., Gałuszka, A., Cearreta, A., Edgeworth, M., Ellis, E. C., Ellis, M. et al. (2016). The anthropocene is functionally and stratigraphically distinct from the holocene. *Science*, *351*, aad2622.

Wieder, W. (2014). Regridded Harmonized World Soil Database v12 Data set. ORNL Distributed Active Archive Center. https://doi.org/10.3334/ORNLDAAC/1247.

Acknowledgements

I want to express my gratitude to my supervisors Michael and Alex for taking the time for the valuable and interesting discussion we had together and for their motivating words and helpful advices. Special thanks goes to Alex for his detailed and frequent feedback. Further, I want to thank Fabian, who was always interested in discussing new approaches and technical details. Also, I wish to thank Jens Kattge for the patient replies to my numerous questions regarding the TRY database. Furthermore I thank my colleagues Moritz and Dominic for the good time we spent together, for the discussions and inputs. I want to thank Elena, who helped me with proofreading of this thesis and was incredible patient and supporting during the sometimes demanding time. Finally, there are my parents, supporting me throughout all my studies and being always there for me. Thank you!

Personal Declaration

I hereby declare that the submitted thesis is the result of my own, independent, work. All external sources are explicitly acknowledged in the thesis.

Place, Date Signature